JOURNAL OF THE AERONAUTICAL SCIENCES

VOLUME 9 DECEMBER, 1941 NUMBER 2

The Propagation of Sound Through the Atmosphere

B. HAURWITZ

Massachusetts Institute of Technology

ABSTRACT

This article gives an elementary survey of the geometrical laws to which sound propagation through the atmosphere is subjected. In a calm atmosphere with decreasing temperature upward, the sound rays are bent upward. If the sound ray returns to the ground, the temperature must increase upward. A wind which becomes stronger with the elevation bends the sound ray back to the ground in the direction of the wind but increases the upward curvature of the sound ray in the opposite direction. Thus, a region of audibility around a source of sound must be asymmetrical if it is due to the wind. Due to the curvature of the sound rays, aircraft can only be heard within a region well above the visual horizon, the so-called acoustical bowl. The zones of anomalous audibility around an explosion which are separated from the region of normal audibility by zones of silence are to be explained by high air temperatures, of about 340° absolute or more, at around 40–50 km. altitude.

INTRODUCTION

THE AIM OF the following article is to give a short survey of the laws to which sound traveling through the air is subjected, and of the bearing which the problem of atmospheric sound propagation has on the audibility of aircraft and on the exploration of altitudes which are, as yet, inaccessible to meteorological soundings by instruments carried aloft by balloons.

GEOMETRICAL ACOUSTICS

The velocity of sound in still air is given by the relation

$$V = \sqrt{\kappa(p/\rho)} \tag{1}$$

where $\kappa = 1.4$, the ratio of the specific heats at constant pressure and at constant temperature, p is the pressure, and ρ is the density of the air. The relation between the pressure and density of dry air can be expressed by the equation of state for ideal gases, since under atmospheric conditions, air behaves like an ideal gas,

$$\rho = pm/RT \tag{2}$$

Received October 14, 1941.

Here T is the absolute temperature, R the universal gas constant, m the molecular weight of (dry) air, $R/m = 2.87 \times 10^6$ cm.^{2}/sec.^{2} deg. The effect of water vapor on the velocity of sound is small and will not be taken into consideration. From Eqs. (1) and (2) it follows that

$$V = \sqrt{\kappa(R/m)T} \tag{3}$$

The velocity of sound depends thus only on the temperature, as long as the composition of the atmosphere does not change. In the latter case, the molecular weight m of the mixture which is called air might become different and κ may assume a different value.

The propagation of sound through the atmosphere is a hydrodynamical problem. Most questions arising in this connection can, however, be treated in a satisfactory manner by a consideration of the sound ray which is normal to the wave surface. The procedure is analogous to the one followed in optics where many problems of the propagation of light waves can be solved by a study of light rays. In analogy to geometrical optics, this method of dealing with the propagation of sound is called geometrical acoustics.

The two factors which affect the propagation of sound in the atmosphere, temperature and wind, change about one hundred times less rapidly in horizontal than in vertical direction. The horizontal variations will therefore be neglected in the following discussion, even though they play, without doubt, a role in producing many of the observable local irregularities of sound propagation. The assumption of purely vertical changes of wind and temperature simplifies the mathematical treatment considerably because the sound ray is then contained in a vertical plane through the sound source, at least as long as the wind direction does not vary with the altitude.

A. The Temperature Effect

To begin with, the propagation of sound in calm air

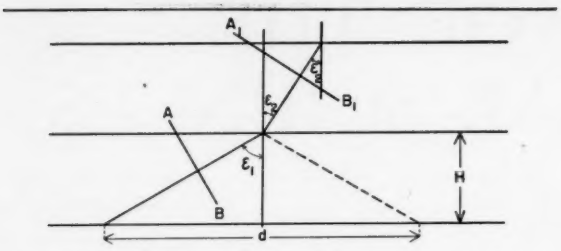

FIG. 1. Refraction of sound rays in a quiet atmosphere.

will be dealt with. In Fig. 1 let the horizontal lines represent the boundaries of two horizontal layers 1 and 2 of the atmosphere. The layers may be so thin that the temperature in each layer can be regarded as constant. If V_1 and V_2 are the velocities of sound in the lower and the upper layer, respectively, and if ϵ_1 and ϵ_2 are the angles of incidence and refraction, it follows in analogy to geometrical optics, that

$$V_1/V_2 = \sin \epsilon_1/\sin \epsilon_2 \tag{4}$$

or

$$V/\sin \epsilon = C \tag{4a}$$

The constant C represents obviously the wind velocity in the layer where the sound ray is horizontal.

The physical effect of a vertical variation of the velocity of sound on the propagation of sound through the atmosphere may be made somewhat clearer by a consideration of the sound as a wave disturbance. Let AB in Fig. 1 represent part of the wave surface. If the sound velocity decreases with elevation, the higher parts of the wave surface will travel more slowly than the lower parts, so that the wave surface, while traveling in a general upward direction, will be turned into the new position A_1B_1. The sound ray which is the normal to the subsequent positions of the wave surface is consequently bent toward the vertical.

Total refraction occurs if $\sin \epsilon_2 \geqq 1$ or if

$$\sin \epsilon_1 \geqq V_1/V_2$$

When the temperature in the lower layer is denoted by T, in the upper layer by $T + \Delta T$, the preceding equation may be written in the form:

$$\sin \epsilon_1 \geqq 1 - (\Delta T/2T) \tag{5}$$

which is sufficiently accurate for practical purposes. Total reflection may therefore occur if the temperature increases suddenly upward (inversion). Table 1 shows the minimum angles of incidence for different intensities ΔT of the temperature inversion.

TABLE 1

Minimum Zenith Angle Necessary for Total Reflection at a Temperature Inversion

ΔT (°C.)	4°	8°	12°	16°	20°
ϵ_1	83°	80°	78°	76°	75°

The temperature below the inversion has been assumed to 280°.

The shortest distance d from the source of sound at which a sound reflected at an inversion at height H returns to the ground is given by (Fig. 1)

$$d = 2H \tan \epsilon_1$$

Substituting from Eq. (5) and neglecting small quantities

$$d = 2H\sqrt{T/\Delta T} \tag{6}$$

If $T = 300°$, $\Delta T = 10°$, $H = 10$ m., it follows that $d = 110$ m. Thus, at 110 m. from the origin of the sound not only is the direct sound wave received, but also the sound ray which is reflected at the inversion.

Inversions are very frequently formed next to the ground on clear calm nights when the surface of the earth cools considerably by radiation. This cooling of the ground is only communicated to the very lowest layers of the air, so that an inversion is formed at low levels. The great audibility of sound during clear calm nights is due to this phenomenon.

If the temperature of the atmosphere does not change suddenly but in a continuous manner, the law of refraction, Eq. (4a), still holds and can be used as a basis for a discussion of the propagation of sound in a calm atmosphere. A rigorous determination of the path of the sound through the atmosphere requires the setting up and integration of the differential equations of the sound ray.[1,2,3] It can be shown, however, that in many cases, especially if the sound ray does not traverse great vertical distances, it is sufficiently accurate to approximate it by a circle. By means of this simple procedure, most of the essential features of the propagation of sound through a stratified medium can be derived. Let the broken curve ABC in Fig. 2 represent part of a sound ray. The horizontal layers

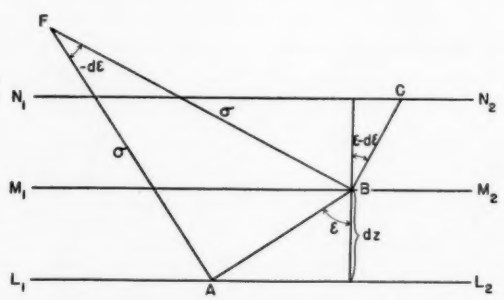

FIG. 2. Radius of curvature of a sound ray.

of the thickness dz between L_1L_2 and M_1M_2 and between M_1M_2 and N_1N_2 may be chosen so small that the velocity of sound can be regarded as constant in each layer. But since the velocity in the upper layer is different from that in the lower layer, the angle which the sound ray makes with the vertical changes

from ϵ to $\epsilon - d\epsilon$ during the passage from the lower to the upper layer. Let AF be perpendicular to AB and BF perpendicular to BC. Then, if the thickness dz of the horizontal strata of air is sufficiently small, it follows that the radius of curvature of the sound ray

$$\sigma = AF = BF$$

except for quantities of higher order. Furthermore, $AB = ds$, the line element of the sound ray, if dz is sufficiently small so that $\sigma d\epsilon = -ds$. Furthermore $ds = dz/\cos\epsilon$, and

$$1/\sigma = -\cos\epsilon(d\epsilon/dz) \tag{7}$$

From Eq. (4a)

$$dV/V = \cos\epsilon\, d\epsilon/\sin\epsilon$$

Thus

$$\sigma = -ds/d\epsilon = dz/\cos\epsilon\, d\epsilon = V\, dz/\sin\epsilon\, dV$$

or

$$\sigma = V/[\sin\epsilon(dV/dz)] \tag{8}$$

If the vertical temperature gradient is constant

$$T = T_0 - \gamma z$$

an assumption which approximates reasonably well the mean state of the troposphere, it follows from Eq. (3) by logarithmic differentiation that

$$(1/V)(dV/dz) = {}^1/_2(1/T)(dT/dz)$$

Thus, for an atmosphere with a linear decrease of temperature

$$\sigma = -(2T/\gamma)(1/\sin\epsilon) \tag{9}$$

In Fig. 3 lines of equal radius of curvature of sound rays are shown in kilometers for different values of the lapse rate of temperature, γ, and of the angle ϵ which the sound ray makes with the vertical. The radius of curvature of the sound rays is smaller, the larger the temperature decrease with the altitude. If $\epsilon = 0$, that is if the ray is vertical, the radius of curvature becomes infinite. This is immediately obvious, since the wave surface is, in this case, horizontal so that all its surface elements travel with the same velocity.

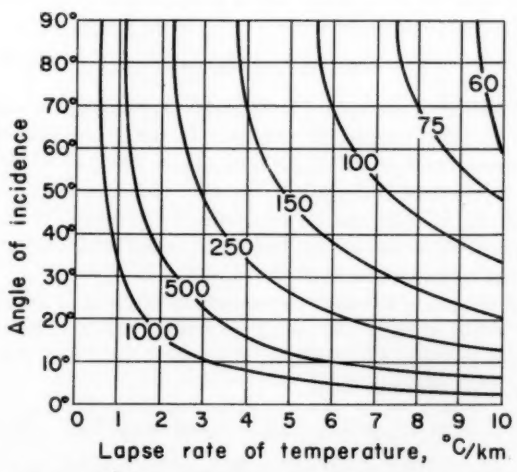

FIG. 3. Lines of equal radius of curvature of sound rays, in km.

After the radius of curvature of the sound ray is obtained from Eq. (8), or from Eq. (9), if the special assumptions made in deriving this equation are satisfied, the sound ray can be constructed with a straight-edge and a compass. It will, of course, in general be necessary to approximate the path of the sound by a number of arcs of circles with different radii and different centers. The center of curvature for a line element of the sound ray is at a distance σ and in a direction perpendicular to the line element, so that the radius makes the same angle ϵ with the horizontal which the sound ray makes with the vertical. On which side of the sound ray the center of curvature is situated can easily be decided, since the sound ray is bent upward when the temperature decreases upward and since it is bent downward when the temperature increases upward. This follows directly from Eq. (4).

It may be added here that the exact calculation gives a cycloid for the sound ray in a calm atmosphere with a linear decrease of temperature. This curve can be approximated by a parabola for numerical computations. But these solutions will not be derived here, since the representation by means of a circle is sufficient to see the essential features of the sound propagation.

B. Wind Effect

If the wind is uniform, the propagation of the sound remains the same as in a still atmosphere except that the whole sound phenomenon is displaced with the velocity of the wind. If the wind changes with the altitude, it will be assumed, following Emden,[1] that the sound is propagated with a velocity equal to the sum of the component of the wind velocity in the direction in which the sound travels plus the sound velocity in still air at the given temperature. To simplify matters, it will further be assumed that the wind is horizontal, that the wind direction does not change, and that the wind varies only in the vertical direction. Under these conditions, the sound rays lie in vertical planes, as mentioned previously.

The effect of a vertical variation of the wind can easily be deduced qualitatively. Consider, for instance, a vertical element of a wave surface traveling in the wind direction in an atmosphere where the wind increases with the elevation. Obviously, the upper part of such an element of a wave surface moves faster than the lower part, so that the normal to the wave surface and also the sound ray are bent downward.

The normal to the wave surface and the sound ray do not coincide any longer when the atmosphere is in motion. A horizontal wave surface, for instance, will travel vertically upward. But, while in an atmos-

phere at rest, each surface element of the wave surface would ascend vertically, it would be displaced horizontally in an atmosphere with a given wind velocity. While the normal to the wave surface does not change its direction, the sound ray is deflected, due to the effect of the wind. The sound ray is, of course, more important than the normal to the wave surface, since the energy transport takes place along the sound rays.

To determine the path of the sound in the atmosphere when a wind of constant direction is blowing, consider Fig. 4. The point A on a sound wave would travel in the unit of time to A' if the atmosphere is at rest.

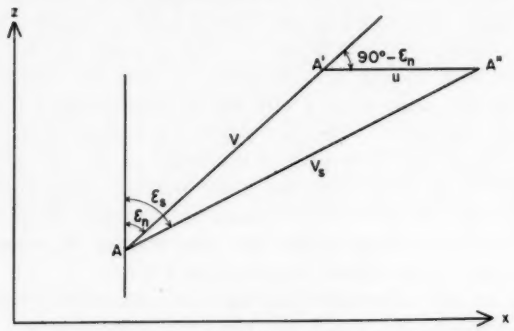

FIG. 4. The effect of wind velocity on the sound ray.

Owing to the horizontal wind velocity u, however, it arrives at A'' after the unit of time has elapsed. AA'' represents the sound ray. If ϵ_n denotes the angle between the normal to the sound surface and the vertical, it follows that the velocity of the sound along the sound ray

$$V_s = \sqrt{V^2 + u^2 + 2Vu \sin \epsilon_n}$$

If ϵ_n denotes the angle between the sound ray and the vertical, it will be seen by taking the projections of V_n and V on the x-axis that

$$V_s \sin \epsilon_s = V \sin \epsilon_n + u$$

Combining the two preceding equations

$$V_s = u \sin \epsilon_s + \sqrt{V^2 - u^2 \cos^2 \epsilon_s}$$

The second term under the square root can, in general, be neglected, since the wind velocity is much smaller than the velocity of sound, so that its square can be neglected in comparison to the square of the velocity of sound. Then

$$V_s = u \sin \epsilon_s + V \tag{10}$$

This equation for the sound ray is only approximately correct, but an analogous relation holds rigorously for the normal to the sound surface.

The law of refraction becomes, in analogy to Eq. (4a)

$$V_s/\sin \epsilon_s = (V/\sin \epsilon_s) + u = C \tag{11}$$

where C is a constant.

For the radius of curvature of the sound ray, the following expression is found using Eqs. (7) and (11):

$$\sigma = -\frac{C - u}{\frac{dV}{dz} + \frac{V}{C - u}\frac{du}{dz}} \tag{12}$$

If the constant C is expressed by the quantities V_0, u_0 and ϵ_0 referring to the height $z = 0$

$$C = (V_0/\sin \epsilon_0) + u_0$$

$$\sigma = -\frac{(V_0/\sin \epsilon_0) + u_0 - u}{\frac{dV}{dz} + \frac{V}{(V_0/\sin \epsilon_0) + u_0 - u}\frac{du}{dz}} \tag{12a}$$

If again a linear vertical distribution of the temperature is assumed

$$(1/V)(dV/dz) = -(\gamma/2T)$$

and if the wind velocity increases linearly with the altitude

$$u = u_0(1 + \alpha z)$$

Substituting in Eq. (12a) it follows that for an atmosphere with constant gradients of temperature and of wind velocity

$$\sigma = \frac{(V_0/\sin \epsilon_0) - \alpha u_0 z}{\frac{V}{2T}\gamma - \frac{V\alpha u_0}{(V_0/\sin \epsilon_0) - \alpha u_0 z}} \tag{13}$$

or

$$\sigma = \sqrt{\frac{T_0}{T}}\frac{(1/\sin \epsilon_0) - (\alpha u_0/V_0)z}{\frac{\gamma}{2T} - \frac{\alpha u_0}{V_0}\left(\frac{1}{\sin \epsilon_0} - \frac{\alpha u_0 z}{V_0}\right)} \tag{13a}$$

At the height $z = 0$ this formula reduces to

$$\sigma_0 = 1/[\sin \epsilon_0(\gamma/2T_0) - (\alpha u_0/V_0)] \tag{14}$$

Eq. (14) will give a sufficiently good approximation to the actual path of the sound ray for small heights. If

$$\alpha u_0 > (V_0\gamma/2T_0)\sin \epsilon_0$$

the radius of curvature is negative so that the sound ray is bent toward the earth. If the lapse rate of temperature $\gamma = 0.6°\text{C}./100$ m., $T_0 = 280°$, $\epsilon_0 = 75°$, an increase of the wind at the rate of 3.5 m./sec. per 1000 m. is sufficient to compensate the effect of the vertical decrease of the temperature for a sound ray in the same direction as the wind.

If the plane in which the sound ray is situated makes an angle χ with the wind direction, the expression $u_0 \cos \chi$ should replace u_0 in Eqs. (13), (13a) and (14). Eq. (14) becomes then:

$$\sigma_0 = 1/[\sin \epsilon_0(\gamma/2T_0) - (\alpha\, u_0 \cos \chi/V_0)] \tag{14a}$$

In order for the sound ray to be bent back to the earth, the radius of curvature must be negative, which requires

that

$$\cos \chi > (\gamma/2T_0)(V_0/\alpha u_0) \sin \epsilon_0 \qquad (15)$$

If the temperature decreases with the altitude, $\gamma > 0$, while the wind velocity increases, $\alpha u_0 > 0$, the right side of Eq. (15) is positive so that the sector in which the sound ray returns to the earth is in the wind direction as was previously found by qualitative reasoning. If the surface temperature is 10°C., the lapse rate of temperature 6°C./km., and the vertical increase of the wind 10 m./sec. for each km., $\cos \chi > 0.358 \sin \epsilon$. If horizontal rays are considered, $\chi < 69°$, so that the sector of audibility has a width of 138°. Outside this sector the sound can only be perceived due to scattering and irregular reflection on the ground.

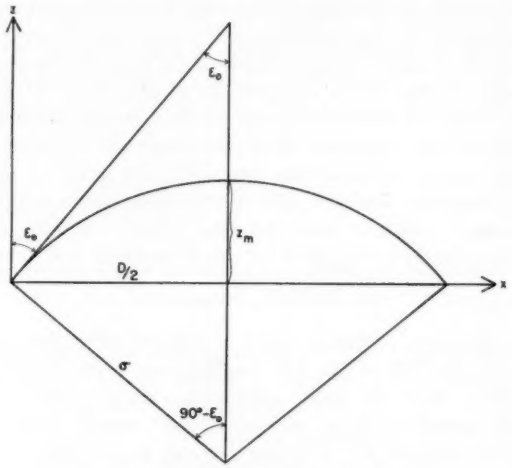

FIG. 5. Path of the sound ray.

To find the path of a sound ray, consider Fig. 5 where the x-axis is horizontal, the z-axis vertical. Let ϵ_0 be the zenith angle of the ray at the source, z_m the maximum height, D the distance at which the ray returns to the surface of the earth. If the ray is regarded as the arc of a circle with the radius σ, it follows that

$$\cos \epsilon_0 = D/2|\sigma| \qquad (16)$$

and

$$z_m = |\sigma|(1 - \sin \epsilon_0) \qquad (17)$$

As indicated in Eqs. (16) and (17), the absolute value of σ should be substituted in these two formulas, since the negative sign of σ has already been taken into account in drawing Fig. 5.

As an example of the effect of wind increase and temperature lapse rate on the propagation of sound, consider an atmosphere with a surface temperature of 10°C. and with the surface wind velocity zero. The temperature may decrease at the rate of 6°C. per km. with the altitude. The wind may increase at the rate of 10 m./sec. per km. in the first three kilometers. This rather large increase of the wind velocity has been chosen in order to show the wind effect more clearly. Above three kilometers the wind may be uniform. Since in an atmosphere with a decreasing temperature upward and without a vertical variation of the wind velocity, the sound ray is bent upward it follows that a sound ray whose maximum height $z_m > 3$ km. will not return to the ground. To find at which distance from the source the sound ray reaching the maximum height $z_m = 3$ km. returns to the ground, the angle ϵ_0 has to be determined. Since the assumed maximum height of a returning sound ray is comparatively small, it may be regarded as a circle. Combining Eqs. (14a) and (17), it follows that

$$\sin \epsilon_0 = \frac{1 - (\alpha u_0 \cos \chi/V_0)z_m}{1 - (\gamma/2T_0)z_m}$$

After ϵ_0 has been found for each ray σ and D can be determined. A sound ray computed in this manner reaches the maximum height from which a sound ray can still return to the ground. The distance D is therefore the maximum distance at which the sound can still be heard except for possible effects of scattering and diffraction. Such a sound ray may be called a limiting ray. Table 2 gives values of ϵ_0, σ, and D for different values of the azimuth χ, the latter being counted from the direction of the wind.

TABLE 2

Limiting Sound Rays Due to Wind Increase with Altitude

χ	ϵ_0	σ	D
0°	70.6°	51.0 km.	34.0 km.
10°	70.8°	52.1 km.	34.2 km.
20°	71.6°	56.4 km.	35.7 km.
30°	72.8°	64.5 km.	38.2 km.
40°	74.6°	80.0 km.	42.5 km.
50°	77.1°	115.0 km.	51.3 km.
60°	80.9°	230 km.	72.9 km.
65°	83.9°	503 km.	113 km.

No sound ray with an azimuth greater than 69° can return to the ground. The distance at which the limiting sound ray returns to the ground becomes very large when the azimuth is around 69°. However, the above table shows that the sound rays are here very nearly horizontal, so that they will be attenuated by irregularities of the earth's surface. At smaller azimuth angles the line connecting the maximum distances for different χ is approximately a straight line. Therefore, regions of anomalous audibility due to an increase of the wind with the elevation have a triangular shape.

If the wind decreases with the altitude, a similar region of audibility is situated in the direction from which the wind is blowing.

When not only the speed of the wind but also its direction changes with the elevation, the conditions become much more complicated. A very detailed study has been published by Galbrun.[4]

The irregularities in the propagation of sound through

the atmosphere are often of great practical importance. To give only two examples: (1) The sound of firing from a gun will be heard better in the direction in which the wind is blowing than in the opposite direction. The wind effect may therefore make the location especially of long-range guns by sound ranging impossible when the wind is blowing from the observer to the battery position. (2) Of two ships, A and B, approaching each other in a fog, the vessel which is downwind, say B, may hear the fog horn of A while its own signal is still inaudible at A. As the vessels approach each other, the signal from B will first be heard on the look-out of A.

The Audibility of Aircraft

When the source of sound is above the earth's surface, as in the case of aircraft, the direction from which the sound seems to come does not coincide with the visual direction owing to the curvature of the sound rays. For the sake of simplicity, it may be assumed first that the source of sound is stationary at the height h, that the atmosphere is calm, and that its lapse rate of temperature γ is constant. The surface temperature may be denoted by T_0. In Fig. 6 let the horizontal through S at the height h above the surface represent the plane in which the aircraft is flying. Assuming

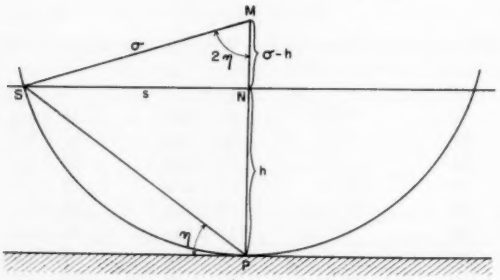

Fig. 6. Range of audibility of an elevated source.

that this height is small enough so that the sound rays can be regarded as circular arcs, an observer on the ground at P will only be able to hear a sound which originates inside a circle which is tangential to the earth's surface at P and whose radius

$$\sigma = -2T/\gamma$$

according to Eq. (9). Therefore, the aircraft cannot be heard at P before it arrives at S. The name "acoustical bowl" has been suggested for the limiting circle with the center M and the radius σ inside which a source of sound must be situated in order to be heard at P.

To an observer at P a sound emanating from S appears to arrive in a horizontal direction while the sound source is seen at an angle η above the horizon. From Fig. 6 it follows that

$$\cos 2\eta = 1 - (h/|\sigma|)$$

Using the above expression for σ, and neglecting small terms, the preceding relation can be simplified to

$$\eta = {}^1/_2 \sqrt{h\gamma/T} \tag{18}$$

For instance, when $h = 3000$ m., $\gamma = 0.6$°C. per 100 m., $T = 280°$, $\eta = 7.2°$.

The horizontal distance SN is given by

$$s = \sqrt{2h\sigma - h^2}$$

or since $h << \sigma$

$$s = 2\sqrt{Th/\gamma} \tag{19}$$

With the previous numerical values $s = 23{,}600$ m.

If the source of sound is moving as in the case of aircraft, there will be an additional displacement of the apparent direction of the sound against the actual direction of the airplane. Let the speed of the aircraft relative to the ground be U. If, further, the height of the airplane above the ground is h and ϕ is the angle of elevation under which it is seen from the ground, its distance from the observer is $h/\sin\phi$. The sound requires the time $h/V_m \sin\phi$ to traverse this distance, where V_m denotes the mean sound velocity between airplane and observer. Thus the airplane will actually be ahead of its sound location by

$$(U/V_m \sin\phi)h$$

In the case of aircraft flying at 1000 m. elevation with a speed of 220 m.p.h., the displacement would be about 300 m. when the sound comes from directly overhead. The actual position of the aircraft would make an angle of about 17° with the vertical, in the direction of travel of the aircraft. There is also a small correction for wind velocity if the atmosphere is not at rest.

If the wind increases with altitude, as is usually the case, the acoustical bowl is, of course, distorted considerably, since the wind bends the sound rays upward in the direction opposite to the wind direction and downward in the wind direction. When the wind direction also changes with the altitude, the problem becomes still more complicated. All those distortions of the acoustical field make a location of the position of aircraft by sound practically impossible, especially owing to the high flying speeds of modern aircraft.

If the wind field does not remain constant but is subjected to irregular variations, the wind propagation through the atmosphere is disturbed in a similar manner. Under such conditions, the sound from the air screw of a passing airplane will appear to be subjected to considerable changes of intensity to an observer at the ground, while in reality the sound energy emitted by the propeller remains constant.

Zones of Silence and of Anomalous Audibility

Occasional observations of sound propagation made during large explosions indicated that apart from the region of direct audibility around the source of sound,

there are other zones of audibility separated from the central region by zones of silence. Systematic studies of this phenomenon were undertaken after the last war, when great amounts of ammunition had to be destroyed. By establishing a network of voluntary observers, it was found that the appearance of zones of silence and of renewed audibility is a regular phenomenon.[4] Fig. 7 shows the distribution of regions of audibility and of silence during an explosion on December 18, 1925, at Kummendorf in Central Germany.

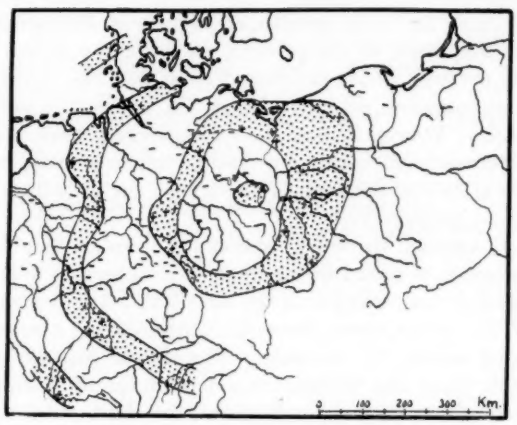

FIG. 7. Zones of anomalous audibility (after Duckert[5]).

The regions of audibility which are separated by zones of silence from the region containing the sound source are called regions of anomalous audibility. In the case shown in Fig. 7 there are indications of more than one zone of anomalous audibility. The existence of more than one zone of anomalous audibility is the rule rather than the exception.

The sound rays which arrive in the zones of anomalous audibility can obviously not have passed along the surface of the earth but must have traveled through higher atmospheric layers. From the preceding discussion, it follows that the wind can hardly produce annular zones of anomalous audibility. When the wind increases with the altitude, the sound rays are refracted back to the earth in the direction downwind while they are bent more steeply upward in the opposite direction. Thus a zone of anomalous audibility produced by the wind would have an asymmetrical appearance. The effect of the wind on the propagation of the sound is indicated by the shape of the region of audibility surrounding the place of the explosion. The extension of this region far toward the east of the source of the explosion and the small width of this region to the west of the explosion indicate a westerly wind in the surface layers which increases with the height.

From the discussion on page 37 it follows that in the atmospheric layers where the temperature, and therefore the sound velocity, decrease with the altitude, the sound rays are bent upward. In order to explain the zones of anomalous audibility, it is necessary to assume that at greater heights the velocity of sound begins to increase again so that the sound rays are refracted or reflected back to the earth.

As long as the wind influence on the propagation of sound is disregarded and as long as the temperature changes only in vertical direction, the sound rays must be symmetrical to their vertices. The velocity of sound at the vertex can be obtained from observations at the ground. Suppose that a number of observing stations at the ground with known distances E from the source of explosion record the time t which the sound needs to travel to the station at the distance E.

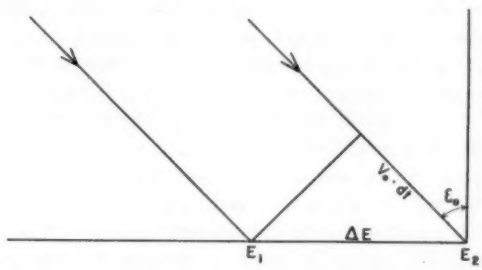

FIG. 8. Determination of sound velocity at the vertex of the sound ray.

By plotting the travel time t *versus* the distance E from the source of explosion, the so-called travel time curve is obtained. In Fig. 8 let E_1 and E_2 be two such observing stations which, for the sake of convenience, are assumed to be on a straight line through the source of the sound and consider two rays returning to the earth's surface at E_1 and E_2. When the wave front reaches the earth's surface at E_1, its position on the ray through E_2 will be given by E_1'. If Δt is the time difference between the arrival of the sound at E_1 and E_2, V_0 the sound velocity at the earth's surface, and ϵ_0 the angle between the vertical and the sound ray, it follows that the distance between E_1 and E_2 can be expressed by

$$\Delta E = V_0 \Delta t / \sin \epsilon_0$$

According to Eq. (4a)

$$\Delta E / \Delta t = V_0 / \sin \epsilon_0 = V / \sin \epsilon = C \qquad (20)$$

$\Delta E / \Delta t$ is given by the direction of the travel time curve. C is the velocity of sound at the level where the sound ray is horizontal, that is, at the vertex of the ray. Thus, the velocity of the sound at the highest point of its path (vertex) can be determined from surface observations. Since the sound velocity at the surface can easily be determined from the surface temperature, Eq. (20) permits also the determination of the angle under which the sound ray arrives at the ground.

The height of the vertex of the sound ray can also be determined. With the aid of the observed dis-

tribution of wind and temperature, the sound ray can be constructed up to the highest point for which aerological observations are available. Above this altitude, somewhat arbitrary assumptions have to be made concerning the meteorological data for the computation of the sound path. But the choice is limited since the travel time and the horizontal distance traveled are known also for the region for which no meteorological data are available. It is even possible to compute the altitude of the vertex of the sound ray by a completely rigorous method, but the approximation method seems to give equally satisfactory results.

From Eq. (20) it follows that the velocity of a sound wave which returns to the earth's surface must be greater at the vertex than at the ground, since the effect of the wind variation cannot account for the anomalous propagation of sound. The vertices of the sound rays which are returning to the ground are, as a rule, at a height of about 40 km. above the ground, at least during the summer over England, according to Whipple.[6] Thus, at these altitudes the velocity of the sound must be considerably greater than near the earth's surface in order to account for the return of the sound rays to the ground.

This increase of the sound velocity is at present generally attributed to a higher temperature of the upper layers of the atmosphere. It will be seen from Eq. (3) that an increase in the velocity of sound could also be brought about by a change of the composition of the atmosphere. If the lighter gases in the atmosphere become predominant at greater altitudes, the molecular weight of the air would decrease, thereby increasing the velocity of sound. However, Wiechert[7] has shown that it would be necessary to assume that already at 40 km. altitude the atmosphere would have to consist of 25 per cent hydrogen in order to account for the sound velocities which must occur at these altitudes. Measurements have shown that up to 20 km. the composition of the air is essentially the same as at the surface of the earth, owing to the pronounced turbulent mixing. Above 20 km. a slight increase in the relative helium content and a decrease of the oxygen content occur according to measurements by Paneth[8] but by far not enough to produce the required increase of the sound velocity at 40 km.

Another factor which might affect the magnitude of the sound velocity is the ratio of the specific heats at constant pressure and at constant temperature, κ. The two main constituents of air in the lower atmosphere, nitrogen and oxygen, are diatomic gases, so that $\kappa = 1.4$. For monatomic gases, on the other hand, $\kappa = 1.67$. It seems unlikely that at the altitude of 40 km. monatomic gases constitute a considerable percentage of atmospheric air, although Chapman[9] has shown that above the level of maximum ozone content (about 25,000 m.) atomic oxygen should become more and more important.

A third possibility, which has been suggested in order to avoid the conclusion that the high sound velocities at upper levels are due to high temperatures, is that Eq. (3) for the sound velocity is not applicable at greater altitudes. The derivation of this formula is based on the assumption that the amplitude of the pressure variation is small compared to the pressure itself. If the amplitude is large, the propagation of the wave is faster, as has been shown theoretically by Riemann and experimentally by observations in the neighborhood of gunfire. It has been argued that, owing to the small pressure at high levels, the ratio of the amplitude of the pressure wave due to sound to the pressure would become so large that the velocity of propagation does not follow Eq. (3) but is much larger. Wiechert[7] has shown, however, that such supersonics do not occur in the upper atmosphere, owing to the decrease of the sound energy with the sound propagation.

It appears, therefore, justifiable to explain the high velocities of sound in the upper atmosphere as due to the high temperatures of the air. Table 3 shows some of the temperatures determined from sound observations during the summer. The second line of this table gives the temperatures determined by Whipple from observations over England, the third and fourth lines give temperatures determined from observations in Germany by Gutenberg and by Duckert.[5] The actual values of the temperature differ, of course, above 30 km., where direct observations cease, but all three authors agree clearly on high temperatures at the levels between 40 and 50 km.

TABLE 3
Summer Temperatures (Absolute) in the Atmosphere from Sound Observations

Height (km.)	20	25	30	35	40	45	50
Whipple	219°	220°	223°	245°	282°	310°	336°
Gutenberg	219°	220°	223°	267°	316°	335°	344°
Duckert	219°	220°	223°	256°	306°	330°	349°

The existence of these high temperatures may be due to the absorption of solar radiation by ozone, as shown by Gowan.[10] The height of the layer of maximum ozone content is actually at about 20–25 km., considerably below the level where the temperature rises according to the sound observations. But Gowan's calculations indicate that the main temperature increase due to ozone absorption takes place above the level of maximum ozone content, in agreement with the observations.

There are, however, certain difficulties connected with this explanation which may be mentioned for the sake of completeness. Anomalous propagation of sound has been observed during 3 out of 12 experimental explosions which were investigated at Russian Arctic stations during the polar night. It appears difficult to explain the anomalous propagation of sound

here by high temperatures in the upper air, since such high temperatures can obviously not be due to direct heating. But it may at least be possible that at these high levels warmer air is continuously transported poleward so that the high temperatures over the Arctic regions would be due to advection from lower latitudes. It does not seem necessary to abandon the explanation of the anomalous propagation of sound by means of high temperatures in the upper atmosphere in view of these observations from Arctic regions.

References

[1] Emden, R., *Beiträge zur Thermodynamik der Atmosphäre*, Meteorol. Zeitsch., Vol. 35, pages 13–29, 74–81, 114–123, 1918.

[2] Milne, E. A., *Sound Waves in the Atmosphere*, Phil. Mag., 6th Ser., Vol. 42, pages 96–114, 1921.

[3] Tucker, W. S., *Some Problems of Modern Meteorology*, No. 11, Meteorological Acoustics, Quart. Journ. Roy. Met. Soc., Vol. 59, pages 203–216, 1933.

[4] Galbrun, H., *Propagation d'une onde sonore dans l'atmosphere*, Gauthier-Villars et Cie, Paris, 1931.

[5] Duckert, P., *Über die Ausbreitung von Explosionswellen in der Erdatmosphäre*, Ergeb. d. kosm., Physik, Vol. I, pages 236–290, Akademische Verlagsgesellschaft, Leipzig, 1931.

[6] Whipple, F. J. W., *The Propagation of Sound to Great Distances*, Quart. Journ. Roy. Met. Soc., Vol. 61, pages 285–308, 1935.

[7] Wiechert, E., *Bemerkungen über die anomale Schallausbreitung in der Luft*, 2 und 3, Mitt., Nachr. Ges. Wiss. Gött., Math.-Nat. Kl., pages 93–103, 201–211, 1926.

[8] Paneth, F. A., *The Upper Atmosphere, Direct Chemical Investigation*, Quart. Journ. Roy. Met. Soc., Vol. 65, pages 304–310, 1939.

[9] Chapman, S., *On Ozone and Atomic Oxygen in the Upper Atmosphere*, Phil. Mag., Ser. 7, Vol. 10, pages 369–383, 1930.

[10] Gowan, E. H., *The Effect of Ozone on the Temperature of the Upper Atmosphere*, Proc. Roy. Soc. Lond., Ser. A, Vol. 120, pages 655–669, 1928; Part II, Vol. 128, pages 531–580, 1930.

Stainless Steel Movable Control Surfaces

GEORGE G. CUDHEA*

Fleetwings, Inc.

Abstract

The general problems affecting the structural design of movable control surfaces are discussed. The need for more adequate specifications for the degree of rigidity of the control surfaces is emphasized. Curves are shown illustrating the effect of hinge location on the weight of dynamically balanced surfaces. The use of light airplane fabric for movable control surfaces is suggested. A short history of stainless steel control surfaces is given. Photographs, weight and dynamic balance data are presented for some typical designs. Deflection data and buckling stresses are shown for tests of ten varying shapes of symmetrical and unsymmetrical leading edge stainless steel nose boxes. The theory of torsion bending of open sections is discussed and has been applied to the results of tests on thirteen nose box cutouts with varying thicknesses and widths of flanges. The specimens tested consisted essentially of simple channels restrained at the ends by three typical leading edge sections. Comparative weight studies are presented for the rudders of two large high speed airplanes as designed in aluminum alloy and stainless steel. Calculations showing the relative strengths, rigidities and weights of these surfaces are included.

Symbols

C_{DB}	= dynamic balance coefficient
x	= drag axis of airplane (+ is aft)
y	= side axis of airplane (+ is to left)
z	= vertical axis of airplane (+ is down)
Σ	= summation
w	= weight
a	= distance along x axis
θ	= angle in radians
T	= torque
G	= modulus of shear
A	= area
s	= periphery
t	= thickness
F_{scr}	= buckling stress
K	= constant
D	= diameter
E	= modulus of elasticity
r	= radius
b	= width
n	= perpendicular distance from shear center
ϕ	= the integral
f	= bending stress
C_{BT}	= constant
e	= distance to the shear center
o	= shear center
h	= height
L	= length (L = 21)
δ	= deflection
J	= torsional rigidity constant
q	= shear stress

Presented at the Structures session, Ninth Annual Meeting, I.Ae.S., New York, January 30, 1941.

* Production Engineer.

Introduction

In the past few years there have appeared numerous papers and articles[1] discussing the application of stainless steel and spotwelding to aircraft structures. These papers discuss the relative merits of 18–8 stainless steel *vs.* aluminum alloy for a broad range of aircraft structures and discuss the comparative physical properties and corrosion resistance of the two materials. The production advantages and low cost of the spotwelding process as applied to stainless steel, have been completely covered and are assumed to be well known.

The purpose of this paper is to present to the designer familiar with aluminum alloy moving control surfaces the proper utilization and limitations of stainless steel when applied to these surfaces. For some types of design, stainless steel is the most efficient; for others, aluminum alloy is best, but in the majority of cases with good design, either material may be effectively used. The major portion of this discussion will be confined to elevators and rudders of airplanes whose design high speeds are in the range of 200 m.p.h. or more. At this point, design loads become of sufficient magnitude so that the design is not based on minimum gage requirements. It should be emphasized that for good strength-weight efficiency in stainless steel, variations in design technique must be made to suit the material.

General Discussion

It is difficult to show the particular application of the material without some general consideration of the design of movable surfaces. During the past few years the author has had the opportunity to examine representative designs from a large number of the aircraft companies in the country. The conviction has gradually grown that a surprisingly large number of control surfaces are not designed—they just happen. While many designs were excellent, few were basically the same with regard to aerodynamic shape and structural detail. Table 1, showing the variation in the important parameters for a representative group, best illustrates the wide difference in opinion existing between aerodynamicists. In preparing this table, an attempt has been made to classify the tail surfaces with reference to the similarity of the particular airplanes. The only apparent aerodynamic agreement seems to exist in the relatively large, fast airplanes.

It is hoped that the conditions apparent from Table 1 become less pronounced as the result of the studies now being conducted by the N.A.C.A.[2, 3, 4]

TABLE 1

Aerodynamic Variation of a Representative Group of Elevators

Design	Area per Side Sq.Ft.	Semi Span—b In.	b^2/A	Aero. Balance %C	Type* Balance	Hinges	T.E. Shape	Speed	Fabric
1	19.7	100	3.5	25	L.E.	Int.	Straight	Fast	Flush
2	28.0	112	3.1	23.5	L.E.	Int.	Curved	Fast	Stitched
3	10.4	83	4.6	14	L.E.	Ext.	Curved	Fast	Stitched
4	11.2	90.3	5.1	20	L.E. and Mod. P.B.	Int.	Curved	Fast	Flush
5	9.3	80.0	4.8	7	P.B.	Int.	Straight	Fast	Stitched
6	14.2	103	5.2	7	P.B.	Int.	Straight	Medium	Stitched
7	9.4	74	4.1	16	L.E.	Int.	Curved	Medium	Flush
8	15.0	81	3.0	22	P.B., L.E.	Ext.	Straight	Medium	Stitched

* L.E. = conventional leading edge, see Fig. 3(*C*). P.B. = paddle balance, see Fig. 3(*A*) and (*B*). Mod. P.B. = modified paddle balance, see Fig. 3(*D*).

The wide differences in structural efficiencies are probably due to the fact that the average weight of the moving control surfaces is only $1^1/_4$ to $2^1/_2$ per cent of the design gross weight, as compared with the wings which range from 10 to 18 per cent. Consequently, the possibilities for reductions in weight in this group have been relatively neglected.

Structural Design Criteria for Moving Control Surfaces

The important factors governing the structural design of moving control surfaces are generally agreed to be:

(a) Strength and loadings
(b) Dynamic balance requirements
(c) Rigidity
(d) Weight and cost

(*a*) *Strength:* The loadings are a function of speed and it is probable that the majority of modern control surfaces have high margins of safety.

(*b*) *Dynamic Balance Requirements:* These are also a function of speed and for most modern airplanes closely approach a requirement of zero. Due to the restrictions now in force the obsolete criteria will be used in the discussion of this subject. Since the basic principles apply regardless of criteria, conversion to any new set of requirements will be simple. It is felt that the present arbitrary requirements, based on the speed vector only, are irrational, and frequently an unnecessarily heavy structural penalty is paid to conform to these requirements. Recent studies[5] indicate that for the probable flutter modes of tail surfaces, adherence to the arbitrary curve of C_{DB} *vs.* speed is not always necessary if the general structural rigidity is high. Despite these studies the requirements have become more severe and an increasingly large proportion of the weight of control surfaces is due to the use of lead for mass balancing. The installation of masses having no structural function, but merely serving the purpose of balancing the control surface, is not considered good practice. It is more desirable to have the leading portion of movable control surfaces sufficiently heavy and rigid so that with light structure and covering in the trailing portion, a sufficient approach to static and dynamic balance will result.

(*c*) *Rigidity:* The available specifications for the rigidity of control surfaces are very loosely written and are expressed as a function of the control system and control surface deflections. The maximum acceptable upper limit for elevators plus control systems is specified as approximately 14 to 15 degrees at the applied loads. The coupling of the control system deflection with the actual surface torsional deflection is irrational. We have two extreme possibilities: very stiff system, very flexible control, and very flexible system, very stiff control. With the former the fundamental vibration frequency of the system will be high and that of the surface low for a given mass balance. With the latter, the fundamental frequency of the control system is low and that of the surface high. Reference 5 indicates that within reasonable limits, the fundamental vibration frequency of the rudder about its own axis is not particularly important, provided that it is sufficiently above that of the rudder control system. For the elevators the possibility of coupling with the fuselage torsion mode requires a relatively high fundamental frequency for elevator unsymmetrical torque. This, of course, presumes adequate stiffness in the fixed surfaces. For lack of anything else in a recent design, the following criteria were established: the calculated deflections were limited to 75 per cent of the total considered acceptable. Half of the deflection was assigned to the control system and half to the surface. In the particular case a satisfactory design resulted.

In general, specifications advise that the torsional rigidity should be as great as possible. This is of little help to the designer who has a wide choice in selecting a type of construction. What the proper rigidity of a control surface should be has not yet been demonstrated. Present designs vary through wide extremes of rigidity with apparently satisfactory results.

(*d*) *Weight* is determined primarily by the preceding three factors, and *Cost* is beyond the scope of this paper except that simplicity of design will naturally result in low cost.

It is felt that in planning the majority of designs, too great emphasis has been placed upon strength, with too little attention given to proper proportions for inherently low dynamic balance coefficients, and to the details such as hinge cutouts and structural discontinuities which, while adequate for strength, produce large deflections.

History of Stainless Steel Surfaces

Stainless steel moving control surfaces are beyond the experimental stage. They have been produced in increasingly large volumes since 1937. There have been in service during the past three years approximately 450 airplanes with these surfaces and it is anticipated that by the end ot 1941 there will be approximately 600 more. The surfaces have been built for unit weights ranging from .9 lb. per sq.ft. to 2 lbs. per sq.ft., the unit weights depending upon the shape, dynamic balance requirements, type of covering (flush or sewed), and, to a limited extent, upon the loadings. In the majority of cases they were built to replace equivalent aluminum alloy surfaces of the same weight.

Table 2

Actual Weights and Dimensions of Some Typical Stainless Steel Surfaces

A	Lead	Unit Wt. Inc. Lead	Balance, %	C_{DB}	Cover	Balance Type
			Elevators			
10.4	3.6	1.93	14.5	.030	Stitch	L.E.
8.10	5.80	2.43	14.5	.025	Flush	L.E.
11.2	3.61	1.80	17.0	0	Flush	L.E.
18.6	0	.87	12.5	.036	Stitch	P.B.
9.4	1.0	1.56	15.5	.032	Flush	L.E.
15.9	2.0	1.28	21.2	.020	Stitch	P.B.
4.54	0	1.10	17.60	.034	Stitch	L.E.
			Rudders			
9.5	4.35	1.86	12.5	.024	Flush	L.E.
12.9	0	1.46	16.5	.034	Flush	L.E.
18.2	2.00	1.19	15.0	0	Stitch	P.B.
19.6	3.06	1.08	...	0	Stitch	P.B.
6.2	0	.91	19.3	.029	Stitch	L.E.

Table 2 lists the important characteristics of a representative group of designs and Figs. 1, 2 and 3 illustrate the types of construction. Figs. 1 and 2 are examples of designs for relatively low speed airplanes, in which the major load-carrying member was either a thin-walled fabricated stainless steel tube or a cold drawn seamless tube. The ribs were simple spotwelded trusses and were attached to the torque tubes by spotwelded

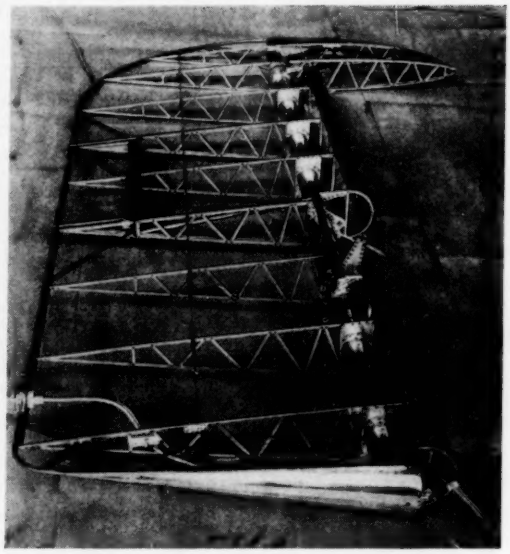

Fig. 1. Early rudder with round fabricated torque tube.

flanged collars. These designs, while very efficient from a weight standpoint, have been superseded for the following reasons: the multiplicity of small parts is undesirable for volume production, and the insert welding required for assembly of the flanges to the tubes, while relatively simple in the factory, is difficult in field service repairs. The additional complication of providing metal fairing for the nose section is uneconomical. Fig. 3 shows examples of modern types of design, with the conventional leading edge nose box so familiar in the aluminum alloy surfaces. Both flush and sewed type surfaces are shown. It is to the design of surfaces of the type shown in the latter group that the remainder of this paper will be confined.

Leading Edge Balanced Surfaces

The most important factor affecting the weight of this type surface is the hinge location. A detailed

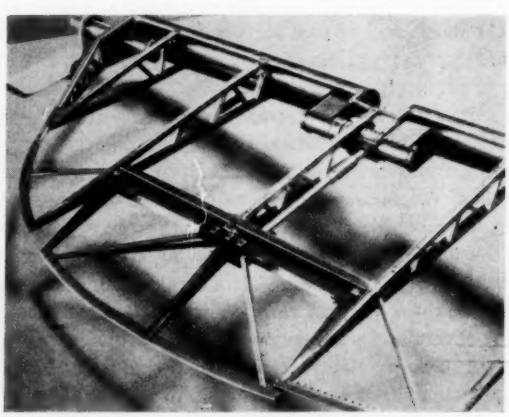

Fig. 2. Elevator with seamless torque tube.

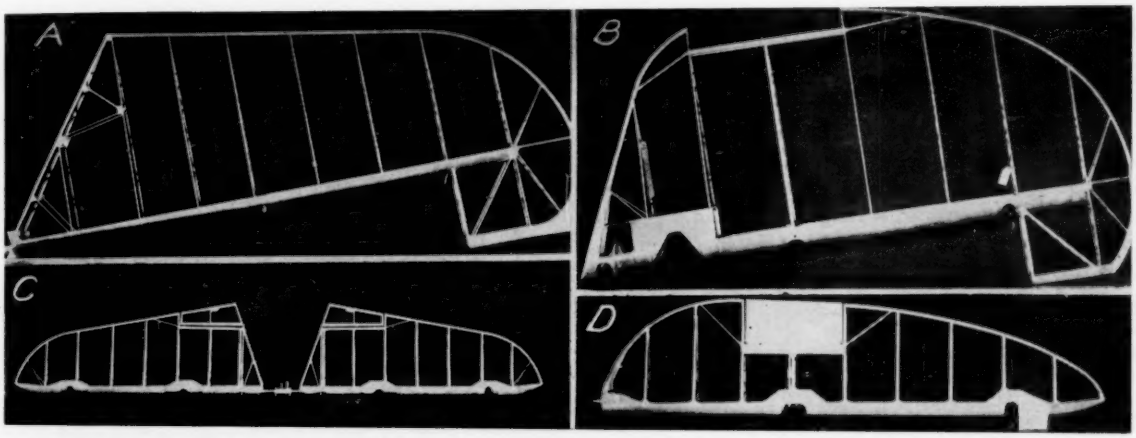

FIG. 3.
(A) Paddle balance elevator with nose box. (B) Paddle balance rudder with nose box. (C) Conventional leading edge elevator with hinge cutouts. (D) Conventional leading edge with modified paddle balance.

study is presented for the elevator shown in Fig. 4. The design is a particularly heavy type since the fabric is flush and the nose box was designed for rigidity rather than strength. The study is presented for the conventional leading edge and for the modified balance shown shaded. Where the product of inertia is calculated for any hinge x, the product of inertia for any other location x_1 is calculated by $\Sigma wx_1y = \Sigma wxy + a\Sigma wy$, where a is the distance in inches between x and x_1. The surface dynamic balance coefficient and product of inertia (less lead) for any location of the hinge is given by the diagonal straight line, Σwxy & C_{DB} *vs.* per cent balance. Reading down from point j, the intersection of a line drawn from the 15.2 per cent balance and the diagonal, we have $\Sigma wxy = 1840$. Reading up from the 1840 point along the dashed curve for the conventional design, or the solid curve for the paddle balance design, the lead required to produce a dynamic balance coefficient of .0235 is determined by the intercept of the curve with the .0235 ordinate, point h for the conventional balance and point k for the paddle balance. Reading across from these intercepts to the abscissa, the lead required for the paddle balance would be 3.5 lbs., for the conventional balance 7.7 lbs. For zero dynamic balance the lead required would be 5.7 lbs. for the paddle balance and 15.2 lbs. for the conventional balance. From the results of this study it is apparent that if increment balance is required a large weight penalty must be paid for hinge locations forward of the 20 per cent line. If, however, increment balance is not required, the balancing mass can be concentrated in the paddle balance and hinge location is not so critical.

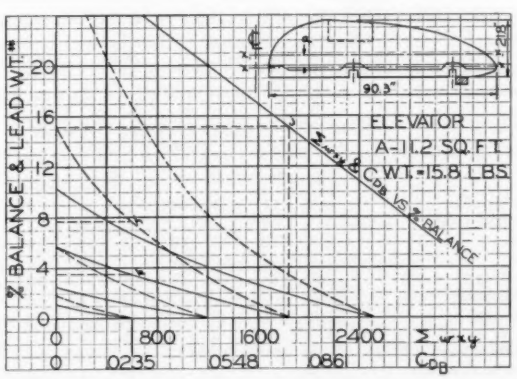

FIG. 4. Curve showing effect of hinge location on dynamic balance for a typical elevator.

This study also illustrates a basic principle in the design of stainless control surfaces. Due to the high density of the material the nose box should be located as far forward as the limitations of nose shape and deflection will permit. The effect of this type design on deflections and strength is discussed later.

Many designers appear to favor a location of 15 to 17 per cent for hinge lines with the idea that the pilot should feel the change in stick forces. While the subject is beyond the scope of this paper, the author wishes to state, after detailed examination of the relatively small difference in stick forces between 10 and 20 per cent balances, indicated by Figs. 13 to 16 of Reference 5, that it is difficult to see how a pilot could distinguish between the feel of a 17 per cent and a 20 per cent balance in the normal operating range.

RIB SPACING AND FABRIC

Ribs

It will be noted from Table 3, that while the ribs and fabric constitute a relatively small percentage of the weight, they contribute the major portion of the adverse wxy. In most designs examined the rib spacing and thread stitching appeared to conform to the curves given in ACM 04. For relatively low speed airplanes this results in a close rib spacing and a consequent

adverse mass distribution. It is believed that these curves were intended for use only with wings. Their use with tail surfaces appears irrational. The comparative design dynamic pressures, at the 35 per cent wing chord and the leading edge of the elevator, for a typical airplane, gave a ratio of 5:1. The maximum practical rib spacing is as a general rule limited by fabric pull and rib attachments to a range of 9–14 in. For the maximum speeds now attainable (V_L = 400 m.p.h.) it is the author's opinion that spacings below 9 in. are unnecessary.

Fabric and Attachments

The present C.A.R. regulations limit the use of light airplane fabric to airplanes with V_D below 150 m.p.h. Here also it is believed that this ruling is intended only for use with wings. Assuming the average dynamic pressure ratio is 4, it would appear practical to use light airplane fabric on moving control surfaces of airplanes, with a V_L of 300 m.p.h. This conclusion is, of course, subject to modification if a very wide rib spacing is used. For the large lightly loaded surfaces shown in Fig. 3 (A and B) the use of light fabric would result in a reduction of 8 per cent in the weight of the control surface group. The reduction would be greater in surfaces with more severe dynamic balance requirements.

Structural Analysis and Design

The stress analysis of the conventional surface is elementary with only three major items to be considered: (a) Ribs, (b) Torque boxes, (c) Hinges and cutouts.

Truss Ribs

Fig. 5 presents the design curves in terms of chord, depth at attachment and average surface load in lbs./sq.ft. for the minimum practical sizes used in spotwelded truss ribs. These curves are the results of 35 tests with a wide range of variables. It is obvious that for the majority of designs the rib size will not be determined by loadings. The curve of weight *vs.* chord was calculated from a large number of representative ribs. The average c.g. of this type of rib is 45 per cent of the chord. Although the rubber press and large production volumes have made this type of rib generally obsolete for aluminum alloy construction, the low cost of spotwelded stainless steel structures makes them economical for quantities less than 500 to 1000 depending on design.

Pressed Ribs

In view of the very thin gages used in stainless steel it is elementary practice to utilize beads and similar reinforcements wherever the part is not exposed to the airflow. This, of course, requires the use of annealed

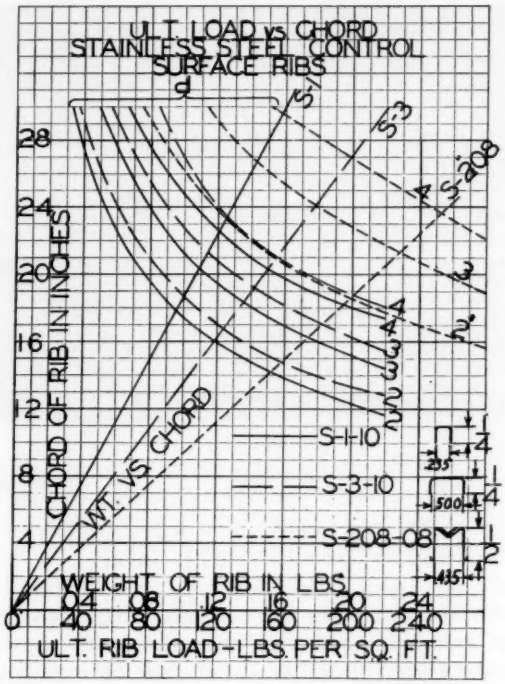

FIG. 5. Curves for selection of design sizes for spot-welded stainless steel truss type ribs.

or 1/4 hard material (u.t.s. 80,000 and 125,000 lbs. per sq.in.). The reduction in tensile strength, however, has very little effect on the strength of ribs since the failures in stamped ribs of very thin gages are normally due to crippling or local elastic instability, and are dependent to a greater extent upon the modulus of elasticity than upon the ultimate tensile strength.

Rubber pressed ribs have already been developed in gages ranging from .006 to .010. The ribs were satisfactory both in strength and rigidity and indicated a substantial decrease in weight for flush types.

TABLE 3

Comparison of Actual Weights and Products of Inertia for Four Typical Surfaces

Type fabric	Stitched		Stitched		Flush		Flush	
Figure	4		3		..		5	
Area	19.57		18.65		12.94		9.42	
Balance and hinge location	Paddle		Paddle	12.5 %	L.E.	17%	L.E.	16%
Weight	18.12		14.85		18.07		12.55	
ΣWxy	2765		3193		1234		813	
	Distribution, %							
Trailing edge	4	17	4	30	4	16	3	30
Tab false spar	1	5	..	..	1	6	1	7
Ribs	7	20	12	28	12	36	12	41
Tab	3	14	..	..	5	29	4	20
Covering	23	63	25	75	12	33	12	38
Tab control	2	3	..	..	3	5	4	4
Nose box	49	− 1	48	− 1	58	−27	61	−44
Fabric braces	1	2	2	3	1	3	1	4
Paddle balance	6	−22	9	−35	..	..	..	..
Horn and brackets	4	..	..	..	4	..	..	..
Unit wts. E/sq. ft.	.93	..	.79	..	1.39	..	1.33	..
C_{DB}	.054	..	.080	..	.037	..	.048	..

TABLE 4 .

Leading Edge Nose Section Test Data

Sections	A	B	C	D	E	F	G	H-1	H-2	H-3
H	...	6.40	2.87	3.62	2.62	3.16	2.90	4.5	6.0	7.5
W	...	5.30	4.20	3.75	2.00	1.90	3.30	3.38	4.50	5.62
R	1.0"	4.0	4.47	3.0	1.25	1.55	7.00	2.25	3.0	3.75
Bulkhead spacing	16	6	8.5	3.5	37.0	22.0	6.0	8.0	10.0	12.0
Enclosed area	3.14	25.67	9.6	11.89	3.97	4.87	6.85	13.01	23.11	36.20
t_w	...	.012	.016	Truss	.030	.030	.0165	.022	.022	.022
t_n	.010	.012	.018	.010	.030	.025	.0165	.022	.022	.022
$(D/t)_n$	200	666	496	600	83.3	124	848	204	272	341
(L/D)	8	.75	.95	.58	14.8	7.1	4.28	1.78	1.67	1.60
(b/t)	...	666	305	550	177	223	194	424	565	706
Buckling—F_{s_1}*	9,800	6700	10,600	8550	20,250	17,800	6,570	19,000	13,700	10,400
Buckling—F_{s_2}*	....	8152	12,130	9090	35,360	44,670	10,135	25,370	19,630	15,615
Buckling—f_s (test)	21,250	6970	12,000	8800	...	...	12,400	19,700	15,020	11,820
Ultimate—f_s (test)	21,250	8010	12,800	9640	...	...	19,000	19,700	15,020	11,820
Remarks	(1)		(2)	(3)	(4)	(5)	(6)			(7)

* F_{s_1} = allowable shear buckling stress using Donnell's short tube formula.
F_{s_2} = allowable shear buckling stress using ANC-5' curved plate formula.

Remarks:
(1) The lap joints in this thin-walled tube had a large effect on the ult. stress.
(2) Poor deflection reading technique.
(3) Truss type shear web gave excessive deflections.
(4) Failure through 1 in. diameter access hole in web.
(5) No failure at f_s = 18,400—test not completed.
(6) Sharp leading edge gave added rigidity.
(7) Deflection curves showed agreement similar to sections H-1 and H-2.

Nose Boxes—Design

It is probable that the majority of nose boxes are designed by the few simple formulas for allowables given in ANC-5. The principles of stress distribution and shear analysis are presented by Kuhn[6] in a readily usable form.

No published data are available which consider the effect of the variations in shape and detail commonly occurring in practice.

A wide range of nose sections have been tested in the conversion of aluminum alloy designs to stainless steel. The results of these tests are presented in Figs. 6 to 8 and Table 4.

These test specimens were in most cases standard production leading edge boxes fabricated from $^1/_2$ hard stainless steel (150,000 u.t.s.). The rear shear webs all had 1 in. diameter access holes for assembly purposes adjacent to the attachment of the nose bulkhead to the web. For closely spaced bulkheads these holes were flanged. The lengths of the specimens were as a rule 36 in. or greater.

The calculated and actual deflections are presented in Figs. 7 and 8. The deflections were calculated using the standard:

$$\theta/l = (T/4GA^2)\int(ds/t)$$

where G = 9,000,000 (effective modulus).

In the presentation of the deflection data the shapes have been classified in two groups: those which conform closely to the theory (Fig. 8), and those varying widely (Fig. 7).

The actual buckling stresses are compared in Table 4 with those calculated using Donnell's cylindrical formula

$$F_{scr} = KE/(D/t)^{5/4}(l/D)^{1/2}$$

and the curved plate formula

$$F_{scr} = 0.1E(t/r) + KE(t/b)^2 \quad (E = 26{,}000{,}000)$$

It was felt that the latter might indicate the effect of the additional stability provided by the shear web.

For the unsymmetrical sections B, C, and D, the actual test deflections are far greater than theory indicates. It is probable that the excessive deflections of specimen D were due to the truss type web.

The symmetrical sections E, F, H-1, H-2 and H-3 agreed closely with the theory up to the torque at which the nose buckles. The apparent agreement shown on the curves is deceptive since G = 9,000,000 was used in the calculated deflections. It has been found in practice that the reduced G accounts for the effect of the access holes in the shear web. The actual G of 18-8 is probably in the range of 11,000,000. Section G while unsymmetrical to a slight degree gave results that were in good agreement.

For specimen A the actual buckling stress is greatly above the calculated due to the effect of the lapped joints.

The use of Donnell's formula is recommended for unsymmetrical sections although the ultimate appears to agree closely with the curved plate formula.

For the H series tests the agreement with Donnell was excellent for the high D/t ratio used. Specimen G carried stresses well above the calculated, the small

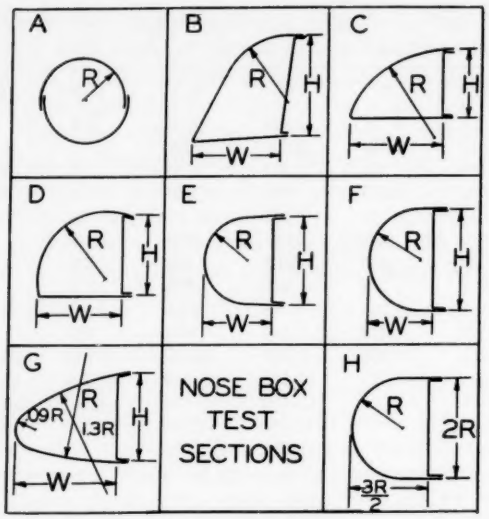

FIG. 6. Sketches of nose box sections tested.

nose radius serving as an effective flange for the diagonal tension fields which formed after buckling. The low D/t ratios of E and F account for the excessive strength.

TORQUE BOX HINGE CUTOUTS

Torsional deflection through hinge cutouts is a major portion of the total deflection of a control surface. This, however, is not apparent from static test reports, since in the majority of reports examined by the author, only the overall deflections of the surface were noted. Deflection readings were taken at only one side of a hinge.

Due to simplicity in assembly the type of cutout shown in Fig. 9 has become standard in stainless steel design. It is essentially a channel restrained at the ends, subject to torque and bending. Several series of tests were made to establish the best distribution of the material and to serve as a basis for deflection calculations through the cutout. There are very few published reports on this subject either from a theoretical or practical viewpoint. There have appeared recently several papers on the effect of torsion on columns,[11] but the solutions suggested are not readily adaptable for the case of simple torsion.

The theory of torsion-bending of open sections has been discussed by J. Lockwood-Taylor.[8] The basic principles of the solution suggested are presented here, adapted to the case at hand. Calculations follow, based on the theory outlined, for the three series of cutouts that have been tested. The application of the method of calculation is discussed and curves are plotted for practical design purposes.

The tests were conducted primarily to justify the design of several production surfaces, and for this reason a larger number of variables were present than desirable for a good theoretical check. Correlation of results within each series of tests is excellent and it seems advisable to present the results of each series separately.

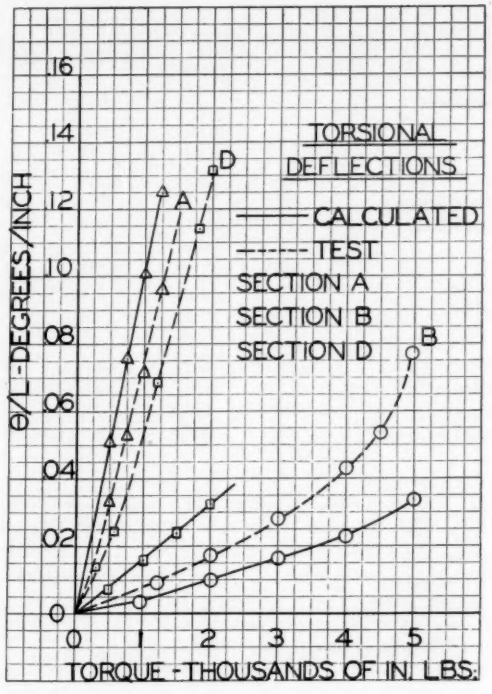

FIG. 7. Torsional deflection curves for unsymmetrical nose box sections.

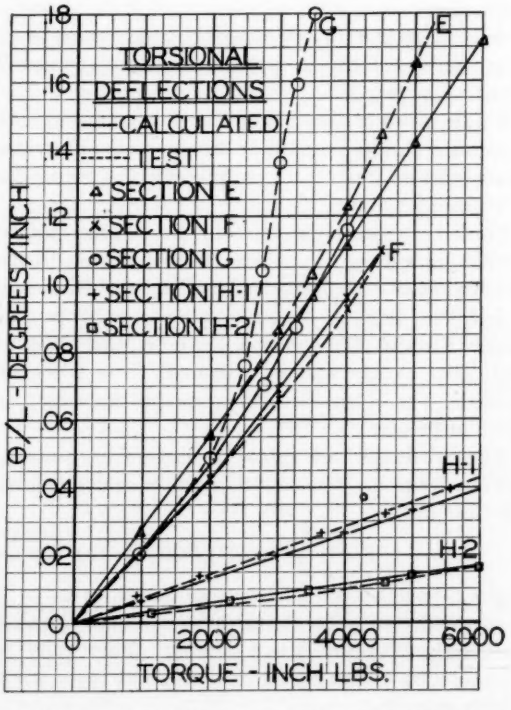

FIG. 8. Torsional deflection curves for symmetrical nose box sections.

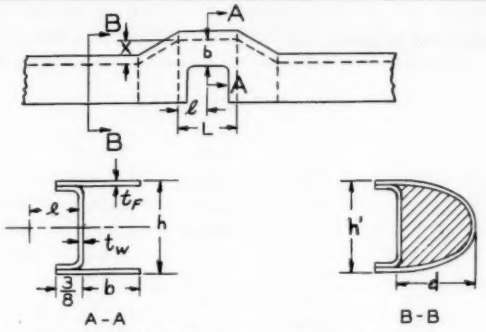

FIG. 9. Sketch of nose box cutout test sections.

A single curve could be plotted for the results of the three series using proper functions of depth of cutout, relative positions of the web, and thickness of the flanges. However, additional tests including a wider range of the variables are necessary before any general equation can be substantiated.

DESCRIPTION OF THE TEST SPECIMENS—(FIG. 9)

Series A test box consisted of a 5 in. long cutout with an offset web and an .065 reinforcement plate added to the flanges of the cutout. The depth of section at the cutout was varied from 3 in. to $1^{3}/_{16}$ in. in four stages.

Series B test box was similar to A except that the offset of the web was $1^{21}/_{32}$ in. instead of $1^{3}/_{8}$ in., and the depth of the web was $2^{1}/_{2}$ in. instead of 3 in. The depth of the section at the cutout was varied from $2^{1}/_{2}$ in. to $1^{1}/_{8}$ in. in four stages. The box was also tested with a $1^{1}/_{8}$ in. depth without any web, and with an .050 web replacing the original .022 web.

Series C test box had no offset of the web, and three tests were run with a constant length (4 in.) and depth of cutout (1.4 in.) and the thickness at the cutout was .065, .050 and .040, respectively. A fourth test was made with a deeper cutout in the .040 material ($1^{1}/_{16}$). The overall length of all specimens was 36 in.

The total deflections through the cutouts are plotted in Fig. 10.

THE THEORY OF TORSION BENDING

"The general St. Venant torsion theory applied to thin open sections, of which a channel is a simple example, gives the result that torsional strength and rigidity are small. While it is true than an open section is much weaker in torsion than a closed section of similar dimensions, subject to certain conditions of end fixity, it is capable of transmitting an appreciable torque with a small deflection. The method of transmission can be described as differential bending of the two flanges. However, when the two members in differential bending form part of a continuous section the conditions are altered somewhat. The general theory applicable to such cases may be called the theory of torsion bending."[8]

The first step in applying the theory to any section is to find the position of shear or the flexural center of the section. For a channel the flexural center lies along the axis of symmetry, and the distance from this point to the web of the channel is noted as e. (See Fig. 9, section A-A.)

$$e = b^2h^2t/4I$$

$$I = 2bt_F(h/2)^2 + (t_wh^3/12) = (bt_Fh^2/2)[1 + (t_wh/6bt_F)]$$

$$e = (b/2)/[1 + (t_wh/6bt_F)]$$

(See Ref. 10.) (Approximate—neglects the $^{3}/_{8}$ in. flange.)

The distribution of bending stress due to torsion is given by the value at any point of the section by the

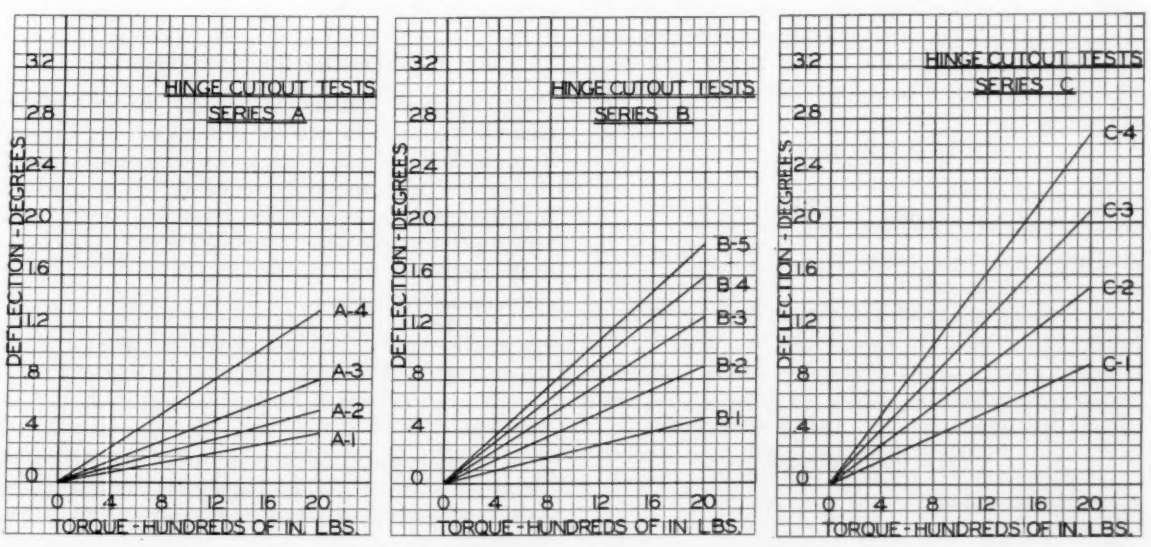

FIG. 10. Torsional deflections of hinge cutout specimens.

TABLE 5

Dimensions and Calculated Deflection for Hinge Cutout

Torque Box Cutout Tests

(a) Parameters of cutouts

Test	L	b	h	t_F	t_w	x	e	C_{BT}	Calc. θ	Test θ	θ_T/θ_c
A-1	5.0	3.03	3.0	.092	.033	2.38	1.44	1.1440	.000703	.0066	9.40
A-2	5.0	2.22	3.0	.092	.033	2.38	1.03	.4728	.001705	.0098	5.74
A-3	5.0	1.62	3.0	.092	.033	2.38	.730	.1935	.00416	.0139	3.34
A-4	5.0	1.18	3.0	.092	.033	2.38	.514	.802	.0101	.0239	2.37
B-1	5.0	2.50	2.47	.092	.022	1.66	.927	.4780	.00168	.0086	5.12
B-2	5.0	1.75	2.47	.092	.022	1.66	.826	.1510	.00533	.0157	2.95
B-3	5.0	1.32	2.47	.092	.022	1.66	.622	.0606	.01330	.0220	1.65
B-4	5.0	1.12	2.47	.092	.022	1.66	.518	.0400	.02010	.0278	1.38
B-5	5.0	1.12	2.47	.092	0	1.66	...	....	.0247	.0322	1.30
B-6	5.0	1.12	2.47	.092	.050	1.66	.469	.484	.0167	.0278	1.66
C-1	4.0	1.40	2.50	.065	.030	0	.615	.0640	.00640	.0160	2.50
C-2	4.0	1.40	2.50	.050	.030	0	.592	.0523	.00785	.0262	3.34
C-3	4.0	1.40	2.50	.040	.030	0	.572	.0449	.00914	.0365	4.00
C-4	4 0	1.06	2.50	.040	.030	0	.407	.0208	.01970	.0468	2.37

(b) Parameters of torque boxes

Series	L'	h'	d	t_B	t_w	Encl. Area	Nose Periphery
A	37	3.20	2.59	.023	.022	6.90	7.0
B	37	2.50	2.88	.023	.022	6.20	7.0
C	45.38	2.50	2.00	.030	.030	4.15	5.5

integral $\int_A n\,ds$ where n is the perpendicular distance from o, the shear center, to the profile. The value of this integral is noted as ϕ.

The distribution of torsion-bending shear, which is connected with the bending stress distribution by a rule similar to that for deriving the ordinary bending shear from the corresponding bending stresses, is given by $\int_B \phi\,ds$. The general equation for the shear distribution is given by

$$(1/t)\int \phi\, t\, ds = (1/t)\int \phi\, dA$$

It remains to evaluate the stress distribution by connecting the stress with the twist of the section, and the latter in turn with the applied twisting moment. The required relation between bending stress and rate of twist is

$$f = E\phi(d^2\theta/dx^2)$$

θ = angle of twist
x = length of member

Similarly, the shear stress is $q = E\int \phi\, ds(d^3\theta/dx^3)$ for uniform thickness.

To connect the twist and torque it is necessary to introduce the quantity C_{BT}, analogous to the rigidity constant usually known as J in the ordinary theory of torsion, and defined by $\int \phi\, dA$, the integral being taken around the whole section. The twisting moment

$$T = EC_{BT}(d^3\theta/dx^3)$$

for a channel section,[10]

$$C_{BT} = \int \phi^2\, dA = (t_w e^2 h^2/12) + (t_F h^2/2)(e^2 b - eb^2 + (b^3/3))$$

By integrating the equation for the twisting moment, the value of θ, the angle of twist is obtained.

Assuming that the ends of the channel are fixed, and the inflection point is at the center of the cutout (equivalent to a free end) integration is taken over the length l. The length l is taken as half the distance between the bulkheads at the ends of the cutout.

Total deflection for L is

$$\theta = TL^3/12EC_{BT} \text{ if } L = 2l$$

The calculations for θ_c for the sections tested are given in Table 5.

DIFFERENTIAL BENDING THEORY

The simplified differential bending theory assumes that all torque is carried by bending in the flanges.[9] Test B-5 was made to check this theory as the web at the cutout was completely removed. It is assumed that the transition from torque to bending occurs at the bulkheads, and the point of inflection is at the center of the cutout.

For a cantilever beam

$$\delta = wl^3/3EI \qquad I = th^3/12 \quad W = T/h$$
$$\tan\theta = 2\delta/(h/2) = 4\delta/h \qquad \tan\theta = 16Tl^3/th^2b^3E$$

Test B-5

T = 2000 in.lbs., l = 2.5 in., t = .092 in., h = 2.47 in., b = 1.12 in., $E = 26 \times 10^6$

$$\tan\theta = .212/h^2b^3 = .0247 \quad \theta_c = 1.4^\circ$$

It will be noted that the portion of the equation for

C_{BT} which accounts for the stiffness of the flanges is of the same form as the differential bending formula.

Assuming $e = b$

$$C_{BT} \text{ (flange)} = t_F h^2/2(b^3/3) = t_F h^2 b^3/6$$
$$\tan \theta = 2Tl^3/3EC_{BT} = 4Tl^3/t_F h^2 b^3 E$$

The theory of torsion bending accounts for the position of o, the torsional center, and includes the rigidity of the web, which is neglected in the differential bending theory.

The theoretical calculation of the torsional deflection through a cutout presented herein is a rational solution of the problem; however, the fixity which the box applies to the cutout is a complex function of several variables. It seems advisable to present the data, Fig. 11, from the first and second series of tests on curves of the ratio of $\theta_{test} \div \theta_{calc.}$ *vs.* b (flange depth at cutout). In the third series thickness, t, replaces b. For design purposes the ratio θ_T/θ_c is considered a fixity factor.

The fixity at the cutout is a function of the carry-over moment along the hinge axis. In the theoretical calculations complete fixity is assumed; however, the test results show that this is not absolutely true but

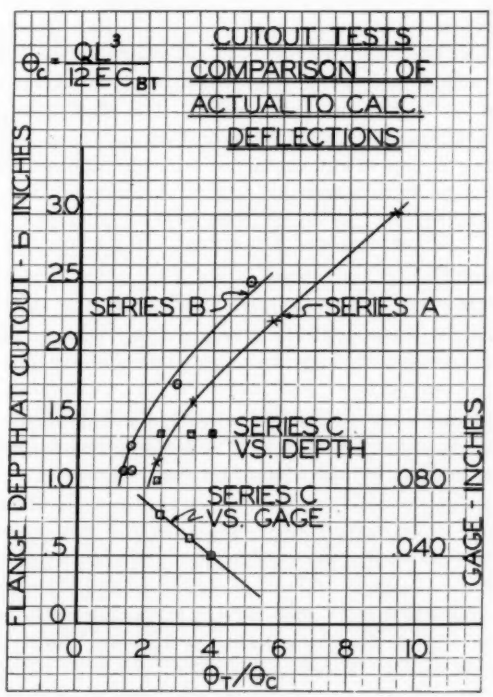

FIG. 11. Comparison of actual and calculated deflections for hinge cutouts.

complete fixity is approached as the depth of flange section at the cutout is decreased. This is obviously true as the rigidity of the box remains constant while the rigidity through the cutout is reduced.

Fixity is also a function of the position of the shear web at the cutout to the shear web at the box. Inspection of the ratio curves of the three series of tests indicates that the fixity is approximately a linear function of this parameter.

The ratio of the gage of the flanges at the cutout to the gage of the torque box is also a parameter of the fixity. The third series of tests substantiates this assumption (Fig. 11). The web gage has a very small effect on the fixity as is indicated by a comparison of tests B-4 and B-6. The depth of cutout for the two tests is the same and the web in B-4 is .022 and in B-6 is .050.

A section has been tested with the web entirely removed, test B-5, as a check on the differential bending theory and an increase of deflection of approximately 10 per cent is noted. This test substantiates the statement in the above paragraph, that the gage of the web has only a small effect upon the fixity and likewise the deflection through the cutout. This agrees reasonably well with the theoretical calculations as noted by a comparison of tests B-4 and B-5 in Fig. 10 (series B).

All tests were continued to 3000 in.lbs. torque with no visible sign of failure or permanent set at the cutout. It is, therefore, concluded that the stresses at the cutout are of little importance for reasonable deflections, and the deflection problem only need be considered.

LARGE CONTROL SURFACES

Design studies for the purpose of conversion to stainless steel were recently made on the group of large aluminum alloy surfaces shown in Table 6. The design specifications required increment static and dynamic balance coefficients of zero. The weights listed for the aluminum alloy surfaces are the actual weights from the manufacturer's detail weight statements. The stainless steel weights are calculated and tend to be conservative. The actual weight of lead used in

TABLE 6

Comparative Weights of Large Stainless Steel and Aluminum Alloy Surfaces

	W_T Struct.	W_T Fabric	Lead and Sup.	Total Wt.	Area	Unit Wt.	ΔW	Des. Load Lbs./ Sq.Ft.
Rudders								
Al. Alloy (A)	29.00	6.82	28.00	63.82	34.1	1.87		65
St. Steel (A)	39.18	6.82	9.00	56.00	34.1	1.62	− 8.82	65
Al. Alloy (B)	29.50	5.60	18.10	53.2	31.00	1.72		52
St. Steel (B)	32.10	6.56	8.84	47.5	31.00	1.53	− 5.7	52
Elevators								
Al. Alloy (A)	12.00	3.95	12.5	28.45	19.74	1.44		100
St. Steel (A)	20.00	3.95	4.50	28.45	19.74	1.44	0	100
Al. Alloy (B)	32.6	5.70	10.00	48.30	28.03	1.71		100
St. Steel (B)	42.30	5.70	...	48.00	28.03	1.71	0	100
Ailerons								
Al. Alloy (A)	20.5	4.20	17.0	41.7	21.0	1.98		53
St. Steel (A)	22.80	4.20	10.0	37.0	21.0	1.76	− 4.7	53
Al. Alloy (B)	27.04	4.60	24.36	56.00	23.75	2.36		35
St. Steel (B)	36.40	4.60	3.00	44.00	23.75	1.85	−12.0	35

TABLE 7

Detail Calculations for Two Sections of Design B

		W	x	W_x	Notes
	Station 40—Rib Spacing 7.5 In.				
Stainless steel	T.E. rib (a)	.325	11.40	3.71	
	T.E. rib (b)	.425	11.40	4.75	
	Tr. edge	.049	36.00	1.76	
	Fabric	.490	12.50	6.12	
	S. web	.252	− 8.00	−2.02	
	Nose rib	.064	− 9.35	− .60	
	Nose skin	.732	− 9.50	−6.95	
	Lead	.297	−10.30	−3.06	
	Total (a)	2.259	.....	−1.04	
	Total (b)	2.359		0	
Aluminum alloy	T.E. rib	.378	8.50	3.20	
	T.E.	.068	36.00	2.45	
	Fabric	.490	12.50	6.12	
	Torque tube	.286	0	0	
	Nose cover	.303	− 5.50	−1.66	
	Nose rib	.036	− 9.35	− .34	
	Lead	.949	−10.30	−9.77	
	Total	2.510	.....	0	
	Station 65—Rib Spacing 5.5 In.				
Stainless steel	T.E. rib (a)	.344	13.50	4.65	Sewed S-3-010
	T.E. rib (b)	.450	13.50	6.07	Flush S-208-008
	T.E.	.040	39.50	1.58	
	Fabric	.360	14.25	5.14	.20 lb./sq.in.
	Shear web	.247	− 8.00	−1.98	.020
	Nose rib	.108	− 8.80	− .95	.015
	Nose skin	.796	− 9.00	−7.12	.040
	Lead	.250	−10.30	−2.57	
	Total (a)	2.145	.....	−1.25	Sewed
	(b)	2.251	.....	+ .17	Flush
Aluminum alloy	T.E. rib	.400	10.40	4.16	.020 Alclad
	T.E.	.050	39.50	1.97	
	Fabric	.360	14.25	5.14	
	Torque tube	.210	0	0	$2^3/_4$−.049 24 ST
	Nose rib	.060	− 8.80	− .53	.020
	Nose cover	.222	− 5.50	−1.22	.016
	Lead	.925	−10.30	−9.52	
	Total	2.227	.....	0	

balancing the aluminum alloy surfaces closely approaches the weight of the structure. This violates the requirements for best design practice noted earlier. In the stainless steel designs an appreciable weight reduction can be noted in most cases. These results were achieved by application of the technique of mass distribution noted earlier. These surfaces had balances ranging from $23^1/_2$ per cent to 25 per cent.

A detail study of the rudders is presented, showing relative strengths of the two designs. The dural surfaces are an interesting illustration of the variation in detail design common in aluminum alloy surfaces. It is believed that the high speeds of both designs A and B were in the same range.

Design A was a conventional aluminum alloy torque box with very narrow hinge cutouts. The shear web was located just aft of the hinge line. Torsional continuity

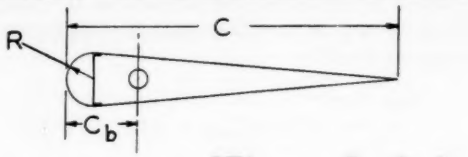

STA.	R	C	C_b
40	3	47	11
65	4	505	11

FIG. 12. Typical large control surface sections, design B.

at the hinges was provided by a short triangular box behind the shear web. The rib spacing was 9 in.

Design B used a $2^3/_4$ in.—.049 24 ST torque tube. The tube was continuous and special bearings were used at the hinges. The leading edge cover was .016 aluminum alloy running to just aft of the hinge line. The rib spacing was 5.5 to 7.5 in. Both designs had pressed ribs with flanged lightening holes.

Table 7 gives the comparative weight and balance studies of the two typical sections for design B, shown in Fig. 12. The stations noted are from the tip. This study neglects the effect of tabs. For the aluminum alloy design the weights and arms are taken directly from the manufacturer's weight report. The lead, however, is that which is sufficient to reduce the static balance coefficient to zero. In the stainless design two rib weights are noted—that for flush attachment, and that for a conventional sewing. The steel nose box sizes were determined by the best arrangement to give a weight equivalent to that of the aluminum surface with zero static balance.

COMPARISON OF STRENGTH AND RIGIDITY

Design B

Ribs: From actual tests of ribs of this size, the strength of the steel rib is 4 or 5 times that required. It is probable that the strength of aluminum alloy rib is also excessive.

Torque Tubes: The actual design torque about the hinge line was 5861 in.lbs. The bending was negligible. The margin for the aluminum tube was 44 per cent: that for the steel, correcting for the forward displacement of the torsional axis, $T = (5861 + 250 \times 9.4 = 8210)$, above 500 per cent from the results of the tests noted in Table 4. The nose radius used in these calculations was 4 in. This surface had a relatively blunt nose. Therefore, to facilitate comparison the sections shown in Fig. 12 were assumed.

Deflections: Fig. 13 gives the approximate design torque and curves for the relative rigidities of the two torque tubes. From this curve the approximate deflection of the aluminum alloy surface is 4.5°. That of the stainless steel is .54°. This neglects the deflection through the middle hinge, but it is apparent from the results of the tests shown in Fig. 10 (series A and C) that the design of a cut-out section to keep the deflec-

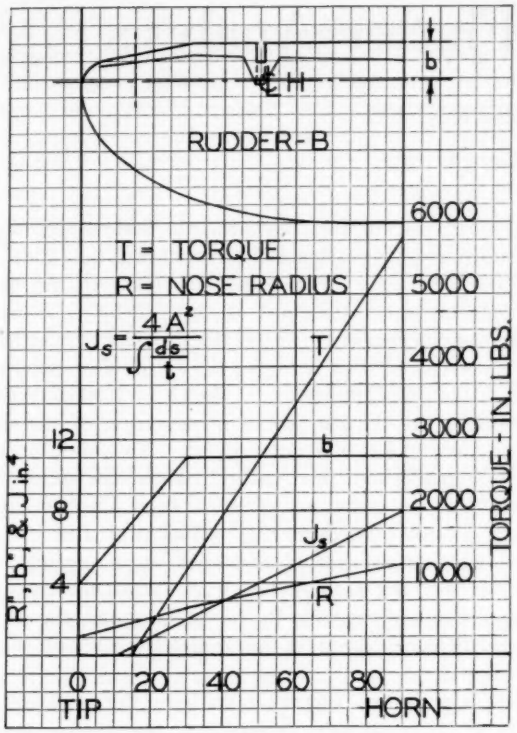

FIG. 13. Loading and deflection data for large control surfaces, design B.

tions below that of the aluminum surface would be simple.

Design A—Rudder

The comparison of a nose box design with a torque tube is definitely unfair since by proper distribution of the material, the same relative efficiency can be obtained in aluminum alloy. Therefore, the rudder designs for A are compared.

The typical nose box design noted in the preceding example was used. The aluminum alloy surface had an .040 skin and web. The steel box had .040 for both. The balance was 25 per cent of the chord. Constant taper ratios were used, therefore, the areas and peripheries of the boxes could be written directly.

Dural:

$$A = R^2[(\pi/2) + 6],\ s = R(\pi + 8)$$

with shear web at 25 per cent chord.

Steel:

$$A = R^2[(\pi/2) + 2],\ s = R(\pi + 4)$$

with shear web at $12^1/_2$ per cent chord where R is the nose radius.

$$J = 4A^2/\int(ds/t) = 4A^2t/s$$

$$\frac{J_aG_a}{J_sG_s} = \frac{(\pi + 12)^2(\pi + 4) \times 3.8 \times 10^6}{(\pi + 8)(\pi + 4)^2 \times 9 \times 10^6} = 1.22$$

This ratio was believed satisfactory as the aluminum alloy design will buckle at a relatively low stress thus changing the comparative rigidity to from 1.22 to .76.

CONCLUSIONS

(a) The present requirements for rigidity are inadequately stated for the designer's use. A wide range of rigidities are possible with the same strength.

(b) The increasing severity of dynamic balance requirements without regard to structural rigidity is unduly conservative.

(c) The location of the hinge line is one of the most important factors affecting the weight of surfaces requiring a low degree of dynamic balance. Every effort should be made to use hinge locations of at least 20 per cent or more.

(d) The use of light airplane fabric for movable control surfaces in the range of speeds higher than that now recommended in ACM 04 should be considered.

(e) The torsion bending theory applied to hinge cutouts of the type described gives a reasonable method for estimating the effect of the various parameters on the deflections.

(f) The principles of mass distribution used in typical stainless designs result in relatively light and rigid surfaces with low inherent products of inertia, when applied to the usual somewhat blunt nose surface. For the best utilization of this principle the maximum ordinate for the nose shape should be well forward of the hinge line.

REFERENCES

[1] *Steel* (Bibliography), Journal of the Aeronautical Sciences, Aeronautical Review Section, pages 40–41, January, 1941.

[2] Goett, H. J., and Reeder, J. P., *Effects of Elevator Nose Shape, Gap, Balance, and Tabs on the Aerodynamic Characteristics of a Horizontal Tail Surface*, N.A.C.A. Technical Report No. 675, 1939.

[3] Silverman, A., and Katzoff, S., *Aerodynamic Characteristics of Horizontal Tail Surfaces*, N.A.C.A. Technical Report No. 688, 1940.

[4] Soule, H. A., *Preliminary Investigation of the Flying Qualities of Airplanes*, N.A.C.A. Technical Report No. 700, 1940.

[5] U.S. Army Air Corps, Materiel Division, *Further Tests of the Single-Tail Flutter Model*, Phase I contd.; *The Critical Flutter Speed as a Function of Control Surface Dynamic Unbalance and Natural Frequencies of Vibration*, Air Corps Technical Report No. 4574, October, 1940.

[6] Kuhn, P., *Some Elementary Principles of Shell Stress Analysis with Notes on the Use of the Shear Center*, N.A.C.A. Technical Note No. 691, March, 1939.

[7] Committee of Aircraft Requirements, ANC-5, *Strength of Aircraft Elements*.

[8] Lockwood-Taylor, J., *The Theory of Torsion-Bending*, Aircraft Engineering, October, 1938.

[9] Timoshenko, S., *Theory of Elastic Stability*, McGraw-Hill, New York, 1936.

[10] Parr, W. S., and Beakley, W. M., *An Investigation of Duraluminum Channel Section Struts Under Compression*, Journal of Aeronautical Sciences, Vol. 3, No. 1, page 21, September, 1935.

[11] Lundquist, E. E., and Flagg, C. M., *A Theory for Primary Failure of Straight Centrally Loaded Columns*, N.A.C.A. Technical Report No. 582, 1937.

[12] U.S. Department of Commerce, Bureau of Air Commerce, *Air Commerce Manual—04*, July, 1938.

Three-Dimensional Flutter Analysis

WILLIAM M. BLEAKNEY*
Lockheed Aircraft Corporation

ABSTRACT

The stability equation for a structure acted upon by air forces is set up in a form convenient for flutter analysis. Unrestricted generalized coordinates in complex form are used. Useful expressions are given for the aerodynamical coefficients of airfoils in terms of theoretical two-dimensional coefficients. The mechanical coefficients for airfoils are expressed in terms of quantities generally known or easily calculable. The value of empirical data from resonance and static-deflection tests is emphasized. The paper is intended as a basis for further development. Detailed steps involved in typical applications will be discussed in a subsequent paper.

INTRODUCTION

THE PURPOSE OF this paper is to present a sound and practical basis for general flutter analysis. It is assumed that the oscillating forces are in effect proportional to the amplitude. Cases of flutter in which this condition probably does not hold, as for airfoils near the stall,[1] constitute another problem. The development applies particularly to streamlined airflow but can be used also in problems involving flow separation and eddies, provided proportionality of the oscillating forces can be assumed. Suspension bridge flutter[2] furnishes an excellent example of such a case.

The calculation of critical flutter speeds of airplanes is difficult, partly because of the extreme complexity of airplane structures, and partly because of our lack of accurate knowledge concerning aerodynamic pressures on oscillating airfoils. The present development allows the analyst to use the two-dimensional flow theory of Theodorsen[3] for each element of span or to alter these theoretical coefficients at will to conform more closely to experience under steady flow conditions and to qualitative considerations arising from the three-dimensional aspects of the problem. New knowledge gained regarding oscillating airflow can be applied at once without complication.

Since adequate experimental verification is lacking (references 4 and 5 give some direct experimental results), the two-dimensional theory must be considered only approximate even for two-dimensional problems. Errors due to airfoil thickness, drag, finite amplitude, compressibility and turbulence must be expected. In three-dimensional problems, the careful analyst must consider, in addition, the effects of taper, aspect ratio, spanwise variation in amplitude, and in some cases aerodynamic interaction between vertical and horizontal surfaces, insofar as the desired accuracy warrants and knowledge and physical intuition allow.

The complexity of airplane structures makes the straightforward application of the principles of mechanics and elasticity to the flutter problem impractical in many cases. For example, neglecting air pressures and structural damping, even the theoretical determination of the normal modes of vibration of a four-engine airplane is a major problem. However, many of these modes and their natural frequencies are easily observable by means of vibration tests after the airplane is built. Furthermore, by means of such vibration tests on completed airplanes, it is possible to predict with fair accuracy the modes and their natural frequencies for airplanes in the design stage, provided these airplanes are not too radically different from those tested.[6]

It is desirable, therefore, to base the mechanical part of these calculations as far as possible on easily observable mechanical characteristics such as normal or primitive vibration modes in still air. Generally a little study will enable one to pick out those modes which are mutually coupled aerodynamically in flight and thus to represent with the fewest possible variables the actual motion involved in flutter. However, it should be borne in mind that forces often are available in flight of sufficient magnitude to produce types of motion which are practically impossible to excite mechanically on the ground. In such cases the analyst must resort to the theory of structures and the results of static tests to determine structural parameters.

From the standpoint of general applicability, it is best to determine the normal modes with control-system motion suppressed, and to investigate the mechanical behavior of the control system by vibration tests and mechanical analyses with fixed-surface motion suppressed. In this way changes in cable tension, cable friction, pilot attitude, etc., do not affect the fixed-surface coordinates, and the effect of high-damping devices in control systems, for example, can be studied with the same system of coordinates as those used on systems with negligible damping. Thus the problem is based on coordinates which are affected only by changes in structural stiffness and weight distribution, and hence are not expected to vary appreciably on any particular airplane except possibly under icing conditions or high static loading.

The practical value of any method of stability estimation is based largely on the generality of the method and the simplicity of the essential operations involved

Received October 3, 1941.
* Research Engineer.

in the solution of problems. These two characteristics have been the primary aim of the present development.

The matrix notation employed by some authors[7,8] is not used, partly because it becomes advantageous in computation only when the number of degrees of freedom is large, and partly because the average engineer is not familiar with its use; the reader, if he so desires, can readily express the equations of this paper in matrix form. The notation of Theodorsen[3] and of Theodorsen and Garrick[9] is followed as far as practicable, considerable care being used to keep it in convenient form for computation work. Some changes are to be expected at a later stage to bring it more nearly in line with accepted usage in other branches of aeronautics.

The convention of signs is such that positive forces are opposed to positive displacements and velocities.

Stability Equation

Consider a structure having n degrees of freedom. Let:

(1) The real functions $f_1, f_2, \ldots f_n$ be normalized deflection modes giving the deflection form associated with each degree of freedom.

(2) The complex numbers $a_1, a_2, \ldots a_n$ specify the relative amplitude and phase of the motion in each degree of freedom. The a's so defined will be referred to as coordinates specifying the motion, the coordinate system being determined by the f's.

(3) The complex functions $\Phi_1, \Phi_2, \ldots \Phi_n$ be aerodynamic force coefficients such that $\Phi_i a_i$ gives the aerodynamic force per unit mass associated with a_i.

(4) The complex functions $F_1, F_2, \ldots F_n$ be the corresponding structural force coefficients.

The f's, Φ's and F's are space vectors. In what follows the products of these vectors are to be interpreted as scalar products.

The equilibrium equation for steady state sinusoidal motion of frequency ω is

$$\sum_j a_j[\Phi_j + F_j - \omega^2 f_j]\,\Delta m = 0 \tag{1}$$

where Δm is an element of mass.

Eq. (1) may now be multiplied by f_i and the result summed over the entire structure. Since the a's are constant over this summation, the result may be written in the form

$$\sum a_j \sum_{\Delta m}[f_i\Phi_j + f_i F_j - \omega^2 f_i f_j]\,\Delta m = 0 \tag{2}$$

It is convenient to introduce the following nondimensional parameters:

$$m_{ij} = (1/\pi\rho b_0^2 S)\sum_{\Delta m} f_i f_j\,\Delta m \tag{3}$$

$$A_{ij} = (1/\pi\rho\omega^2 b_0^2 S)\sum_{\Delta m} f_i\Phi_j\,\Delta m \tag{4}$$

$$\bar{\Omega}_{ij} = \sum_{\Delta m} f_i F_j\,\Delta m/\omega_0^2\sum_{\Delta m} f_i f\,\Delta m \tag{5}$$

$$X = \omega_0^2/\omega^2 \tag{6}$$

where ρ is the air density, ω_0 is a reference frequency, and b_0 and S are, respectively, the reference lengths in the direction of, and transverse to, the airstream. The set of Eqs. (2) may now be written in the form

$$\begin{aligned}&[A_{11} - m_{11}(1 - \bar{\Omega}_{11}X)]a_1 + \\ &\qquad [A_{12} - m_{12}(1 - \bar{\Omega}_{12}X)]a_2 + \ldots = 0\\ &[A_{21} - m_{21}(1 - \bar{\Omega}_{21}X)]a_1 + \\ &\qquad [A_{22} - m_{22}(1 - \bar{\Omega}_{22}X)]a_2 + \ldots = 0\end{aligned} \tag{2'}$$

The relation to be satisfied by the coefficients for a steady state solution is then the determinantal equation:

$$\begin{vmatrix} A_{11} + M_{11} & A_{12} + M_{12} & \ldots & A_{1n} + M_{1n} \\ A_{21} + M_{21} & A_{22} + M_{22} & \ldots & A_{2n} + M_{2n} \\ \cdot & \cdot & & \cdot \\ \cdot & \cdot & & \cdot \\ \cdot & \cdot & & \cdot \\ A_{n1} + M_{n1} & A_{n2} + M_{n2} & \ldots & A_{nn} + M_{nn} \end{vmatrix} = 0 \tag{7}$$

where

$$M_{ij} = -m_{ij}(1 - \bar{\Omega}_{ij}X) \tag{8}$$

The only assumption made in the above development is that of complete linearity. Actually a great deal of information can be obtained about the behavior of systems far beyond the linear range by the use of effective or average parameters determined experimentally or otherwise. For example, it is sometimes possible to estimate the flutter amplitude at a given air speed by finding the amount of damping required to maintain a steady state, or to distinguish between gradual and explosive types of flutter by the rate at which this calculated damping term increases with air speed.

Aerodynamic Coefficients

In the determination of the A's in Eq. (7) by means of Eq. (4) it is usually possible to neglect the aerodynamic forces on all surfaces except airfoils. Forces normal to the plane of the airfoil, according to Eq. (4), combine only with the component of f in this direction. With the assumption of no chordwise deformation except at breaks between surfaces this component may be expanded in the form

$$f_i = h_i + x\alpha_i/b_0 + r\beta_i/b_0 + s\gamma_i/b_0 \tag{9}$$

where x is the distance aft of the quarter chord, r the distance aft of the first hinge, and s the distance aft of the

second hinge. Eq. (9) defines the quantities h_i, α_i, β_i and γ_i, which will be referred to as "weighting factors." The quantities β_i and γ_i have values on the first (including the second) and the second movable surfaces, respectively, and are zero elsewhere.

The above expansion is useful in the calculation of m_{ij}. The general equation in terms of the weighting factors is given below (Eq. 14). For the calculation of A_{ij} it is convenient to introduce the following weighting factors:

$$h_i' = h_i b/b_0;\ \alpha_i' = \alpha_i b^2/b_0^2;\ \beta_i' = \beta_i b^2/b_0^2;\ \gamma_i' = \gamma_i b^2/b_0^2 \tag{10}$$

where b is the half chord.

In two-dimensional problems aerodynamic coefficients are defined by expressions for the lift forces and moments per unit of span as follows:

$$\begin{aligned}
\text{Lift} &= \pi\rho b^3\omega^2[(h/b)A_{ch} + \alpha A_{c\alpha} + \beta A_{c\beta} + \gamma A_{c\gamma}] \\
\text{Quarter-chord moment} &= \pi\rho b^4\omega^2[(h/b)A_{ah} + \alpha A_{a\alpha} + \beta A_{a\beta} + \gamma A_{a\gamma}] \\
\text{First-hinge moment} &= \pi\rho b^4\omega^2[(h/b)A_{bh} + \alpha A_{b\alpha} + \beta A_{b\beta} + \gamma A_{b\gamma}] \\
\text{Second-hinge moment} &= \pi\rho b^4\omega^2[(h/b)A_{dh} + \alpha A_{d\alpha} + \beta A_{d\beta} + \gamma A_{d\gamma}]
\end{aligned} \tag{11}$$

where h, α, β and γ, expressed in terms of magnitude and direction on the complex plane, give the amplitude and phase of the motion of the quarter-chord point normal to the plane of the airfoil, the rotation about a spanwise axis, the first hinge angle, and the second hinge angle, respectively. Theoretical expressions for nine of the above coefficients are given in reference 9. Five others, $A_{c\gamma}$, $A_{a\gamma}$, A_{dh}, $A_{d\alpha}$ and $A_{d\gamma}$, can be written down at once from these expressions, making use of the second hinge position instead of the first. Only $A_{b\gamma}$ and $A_{d\beta}$ require separate derivation. It should be noted that Theodorsen's coefficients include mechanical effects and are referred to the elastic axis, while in the present development the two-dimensional A's depend only upon aerodynamic parameters such as hinge position and "reduced frequency," and the reference axis is taken at the aerodynamic center.

Using the definitions involved in Eqs. (1), (9) and (10) Eqs. (11) become

$$\begin{aligned}
\text{Lift} &= a_j\sum_{\Delta m}\Phi_j\,\Delta m = a_j\pi\rho b b_0\omega^2[h_j'A_{ch} + \alpha_j'A_{c\alpha} + \beta_j'A_{c\beta} + \gamma_j'A_{c\gamma}] \\
\text{Quarter-chord moment} &= a_j\sum_{\Delta m}x\Phi_j\,\Delta m = a_j\pi\rho b^2 b_0\omega^2[h_j'A_{ah} + \alpha_j'A_{a\alpha} + \beta_j'A_{a\beta} + \gamma_j'A_{a\gamma}] \\
\text{First-hinge moment} &= a_j\sum_{\Delta m}r\Phi_j\,\Delta m = a_j\pi\rho b^2 b_0\omega^2[h_j'A_{bh} + \alpha_j'A_{b\alpha} + \beta_j'A_{b\beta} + \gamma_j'A_{b\gamma}] \\
\text{Second-hinge moment} &= a_j\sum_{\Delta m}s\Phi_j\,\Delta m = a_j\pi\rho b^2 b_0\omega^2[h_j'A_{dh} + \alpha_j'A_{d\alpha} + \beta_j'A_{d\beta} + \gamma_j'A_{d\gamma}]
\end{aligned} \tag{12}$$

the summation being taken over the chord.

The above expressions can be used in three-dimensional problems provided oscillations in the spanwise component of airflow can be neglected, for then two-dimensional airflow theory can be used to determine the pressure on each element of span. However, in practical airplane problems this assumption often cannot be made. In order to approach actual physical conditions without seriously complicating the analysis the assumption is proposed that the above equations are correct with respect to phase and chordwise distribution of pressure and in error only in magnitude. With this assumption it is sufficient to replace h_j', α_j', β_j' and γ_j' in Eqs. (12) by the new weighting factors h_j'', α_j'', β_j'', and γ_j'', the difference accounting for the change in the oscillating pressure due to spanwise flow effects. The new equations will be referred to as Eqs. (12′). Pressure data under steady-flow conditions can in some cases be utilized to estimate the difference between the primed and double-primed factors, and qualitative physical considerations are in many cases sufficient for a good approximation. For example, it is known that differential pressures must approach zero near airfoil tips, that a small tab will affect the pressure distribution on a wing over a much greater span than that of the tab itself, and that lateral pressures on twin vertical tail surfaces are affected by the elevator hinge angle and the angle of attack of the horizontal surface.

If definite information is available showing that the above assumptions are incorrect, it is possible to allow for the actual spanwise effects by giving the weighting factors a complex character and using different factors in each of the four Eqs. (12′).

Finally, Eqs. (4), (9), (10) and (12′) may be combined as follows:

$$\begin{aligned}
A_{ij} = \sum_{\Delta y}[&\alpha_i'\alpha_j''A_{a\alpha} + \alpha_i'h_j''A_{ah} + \alpha_i'\beta_j''A_{a\beta} + \alpha_i'\gamma_j''A_{a\gamma} + h_i'\alpha_j''A_{c\alpha} + h_i'h_j''A_{ch} + h_i'\beta_j''A_{c\beta} + h_i'\gamma_j''A_{c\gamma} \\
&+ \beta_i'\alpha_j''A_{b\alpha} + \beta_i'h_j''A_{bh} + \beta_i'\beta_j''A_{b\beta} + \beta_i'\gamma_j''A_{b\gamma} + \gamma_i'\alpha_j''A_{d\alpha} + \gamma_i'h_j''A_{dh} + \gamma_i'\beta_j''A_{d\beta} + \\
&\gamma_i'\gamma_j''A_{d\gamma} + l_i l_j D\sqrt{-1}/\pi b_0 k_0]\,\Delta y/S
\end{aligned} \tag{13}$$

where Δy is an element of span. The last term is added for completeness, although it is seldom of any importance. The quantity l_i is the chordwise component of f_i, D is the drag coefficient such that the chordwise drag per unit span is $\rho v^2 D/2$, and $k_0 = b_0\omega/v$. For the coordinate systems usually chosen more than four terms rarely occur on the right of any one equation of the set (13).

Inertial Parameters

For the calculation of the inertial parameters there is no difficulty in applying Eq. (3) directly. The summation, of course, should include all moving structure, taking account of the vector character of the f's.

In the case of airfoils, data are usually obtained in the form of mass, center of gravity position, and radius of gyration of chordwise sections of the airfoil and movable surfaces. The contribution to m_{ij} of such a section is easily obtained by combining Eqs. (3) and (9) and integrating over the chord. The result may be expressed in the form

$$\Delta m_{ij} = \frac{\Delta y}{\pi \rho b_0^2 S}\left\{\left[\frac{x_0^2 + r_0^2}{b_0^2}\alpha_i\alpha_j + \frac{x_0}{b_0}\left(\alpha_i h_j + h_i\alpha_j\right) + h_i h_j\right] w + \left[\frac{c_1 x_\beta + r_\beta^2}{b_0^2}\left(\alpha_i\beta_j + \beta_i\alpha_j\right) + \frac{x_\beta}{b_0}\left(h_i\beta_j + \beta_i h_j\right) + \frac{r_\beta^2}{b_0^2}\beta_i\beta_j\right] w_\beta + \left[\frac{c_2 x_\gamma + r_\gamma^2}{b_0^2}\left(\alpha_i\gamma_j + \gamma_i\alpha_j\right) + \frac{x_\gamma}{b_0}\left(h_i\gamma_j + \gamma_i h_j\right) + \frac{(c_2 - c_1)x_\gamma + r_\gamma^2}{b_0^2}\left(\beta_i\gamma_j + \gamma_i\beta_j\right) + \frac{r_\gamma^2}{b_0^2}\gamma_i\gamma_j\right] w_\gamma\right\} \quad (14)$$

---

where

- c_1 = x-coordinate of the first-hinge center line.
- c_2 = x-coordinate of the second-hinge center line.
- x_0 = x-coordinate of the center of gravity of the total airfoil section.
- $c_1 + x_\beta$ = x-coordinate of the center of gravity of the first movable section (including the second).
- $c_2 + x_\gamma$ = x-coordinate of the center of gravity of the second movable section.
- r_0 = radius of gyration of the total airfoil section about its center of gravity.
- r_β = radius of gyration of the first movable section (including the second) about the first-hinge center line.
- r_γ = radius of gyration of the second movable section about the second-hinge center line.
- w = mass per unit span of the whole airfoil.
- w_β = mass per unit span of the first movable surface (including the second).
- w_γ = mass per unit span of the second movable surface.

It is obvious from Eq. (3) that the inertial parameters are symmetrical, that is,

$$m_{ij} = m_{ji} \quad (15)$$

Diagonal Structural Parameters

It is convenient to separate the real and imaginary parts of $\bar{\Omega}_{ii}$ as follows:

$$\bar{\Omega}_{ii} = \Omega_i(1 + g_i\sqrt{-1}) \quad (16)$$

Since the real part of F_i determines those structural forces associated with the ith mode which are in phase with the displacement, the maximum potential energy for the notation a_i alone is given by

$$(1/2)|a_i^2|\sum_{\Delta m} f_i F_i \text{ (real)}\ \Delta m \quad (16a)$$

The maximum kinetic energy is

$$(1/2)|a_i^2|\omega^2\sum_{\Delta m} f_i^2\,\Delta m \quad (16b)$$

The frequency ω_i at which these two quantities are equal is called the primitive frequency. By Eqs. (5) and (16)

$$\Omega_i = \omega_i^2/\omega_0^2 \quad (17)$$

If the ith mode is a natural mode, ω_i is easily observed by means of resonance tests provided the damping is not too high. Furthermore, by suppressing other modes by means of rigid restraints so that the energy supplied by the restraints is zero, primitive frequencies that are not natural for the original structure often can be observed by means of resonance tests.

Another method of great practical value consists in applying Eq. (7) to the conditions prevailing during resonance tests. For this purpose it is usually possible to neglect the imaginary part of the coefficients and to find, by trial, a set of values of Ω_i for which the solutions for X agree with the observed resonant frequencies. It should be noted that for still air the aerodynamic coefficients may not be negligible since aerodynamic inertial effects are often considerable. Theoretical values can be found by putting the "reduced wave length" $1/k$ equal to zero in Theodorsen's coefficients.[9] Strictly speaking ω_i is the primitive frequency *in vacuo*.

When vibration data are not available well known methods from the theory of elastic structures make it possible to calculate the strain energy in most cases.[10] In the case of pure bending along the y-axis, for example, it is easily shown that

$$m_{ii}\Omega_i = \frac{1}{\pi \rho b_0^2 S\omega_0^2}\sum_{\Delta y} EI\left(\frac{d^2 h_i}{dy^2}\right)^2 \Delta y \quad (18)$$

where EI is the usual flexural modulus. Similarly, in the case of pure torsion, where KG denotes the torsional modulus,

$$m_{ii}\Omega_i = \frac{1}{\pi\rho b_0^4 S\omega_0^2}\sum_{\Delta y} KG\left(\frac{d\alpha_i}{dy}\right)^2 \Delta y \qquad (19)$$

In complex cases where deflection under load cannot be predicted satisfactorily by analytical methods and a flutter analysis is required while the structure is still in the design stage, it is sometimes possible to make good estimates, either of the primitive frequency from statistical studies of resonance tests on similar structures, or of the strain energy from static load-deflection data on similar structures.

The quantity g_i defined by Eq. (16) is called the damping factor for the ith mode. The set of values for g_i completely determines the energy dissipated in the structure. Each value is numerically equal to the tangent of the phase angle by which the generalized structural force leads the displacement in the corresponding mode. These values are most easily determined by means of vibration tests. A common means of exciting vibration makes use of the inertial reaction of a reciprocating or rotating weight. If ϵ is the unbalance of such an exciter, the amplitude of the exciting force is $\epsilon\omega^2$.

Consider the exciter mounted on a structure on which all modes except the ith are suppressed. While the suppression is not always feasible it can often be done with little difficulty during a test by applying rigid restraints at points along the nodes of the ith mode. Under these conditions Eqs. (2′) are replaced by the set

$$(A_{ji} + M_{ji})a_i = \frac{\bar{\epsilon} f_{je}}{\pi\rho b_0^2 S} + \sum_r \frac{\overline{R}_r f_{jr}}{\pi\rho b_0^2 S\omega^2} \qquad (20)$$

where f_{je} is the value of f_j at the position of the exciter, f_{jr} is the value of f_j at the position of a given restraint, $\overline{R}_r$ is the force acting at that restraint, and $\bar{\epsilon}$ is given a complex character to indicate the phase of the exciter. Since a_i and all quantities on the right are either known or measurable the set of Eqs. (20), in principle, will yield all mechanical parameters provided the A's can be either neglected or determined by other means. In practice the method is not generally applicable because of the complexity of the experimental setup and suppression difficulties. However, the equation for which $j = i$ is useful for determining damping factors since in this case the summation on the right vanishes because of the condition that the ith mode is not affected by the restraints. If aerodynamic effects are neglected

$$M_{ii} = -m_{ii}(1 - \Omega_i X) + m_{ii}g_i\Omega_i X\sqrt{-1} = \frac{\bar{\epsilon} f_{ie}}{\pi\rho b_0^2 S a_i} \qquad (21)$$

Elimination of $\Omega_i X$ yields

$$g_i = \sin\theta/[\cos\theta + \pi\rho b_0^2 S m_{ii}|a_i|/\epsilon f_{ie}] = \sin\theta/[\cos\theta + (\sum_{\Delta m} A^2\Delta m)/\epsilon A_e] \qquad (22)$$

where θ is the angle by which the exciter leads the coordinate a_i, $A = |a_i| f_i$ is the amplitude of the motion of the structure, and A_e is the value of A at the exciter. At the primitive frequency

$$g_i = \epsilon f_{ie}/|a_i|\sum_{\Delta m} f_i^2\Delta m = \epsilon A_e/\sum_{\Delta m} A^2\Delta m \qquad (23)$$

If a constant-force exciter is used ϵ should be replaced by the amplitude of the force divided by ω^2. In the application of Eq. (23) it is usually sufficient to determine the maximum response only. Any error due to a value of θ different from 90° will then be on the conservative side.

Two other methods are frequently used for the determination of damping factors.[11] The first follows from Eq. (21) if the absolute values of the left and right members are used. The amplitude $|a|$ is proportional to $[(1 - \Omega X)^2 + \Omega^2 X^2 g^2]^{-1/2}$ for the "inertia exciter" and $[(1 - 1/\Omega X)^2 + g^2]^{-1/2}$ for an exciting force independent of frequency, the subscripts being omitted since only one degree of freedom is considered. In both cases by straightforward, although somewhat lengthy, manipulation it follows that

$$g = (X_1 - X_2)/(X_1 + X_2) = (\omega_2^2 - \omega_1^2)/(\omega_2^2 + \omega_1^2) \qquad (24)$$

where ω_1 and ω_2 are the frequencies at which the amplitude is $1/\sqrt{2}$ times the maximum amplitude and g is assumed independent of frequency.

A third method makes use of the decay curve for free vibration. Since the motion in this case is definitely non-sinusoidal and the mechanism of damping often quite complicated and frequently unknown, it is best to consider the motion from the energy standpoint. It is easily shown that for steady motion the energy dissipation per cycle is $2\pi g$ times the vibrational energy. It is reasonable to assume the same law for free vibration, that is, that the energy decrease from one displacement maximum to the next is $2\pi g$ times the average potential energy at these two instants. Assuming the potential energy is proportional to the square of the displacement it follows that

$$\pi g = (a_n^2 - a_{n+1}^2)/(a_n^2 + a_{n+1}^2) \qquad (25)$$

for the nth and $(n + 1)$th displacement maxima. In case the damping is small it may be assumed constant over a large number of cycles and Eq. (25) may be written approximately in the form

$$g = (1/\pi n)\log_e (a_0/a_n) \qquad (26)$$

for a series of n cycles.

Of the three methods represented by Eqs. (23), (24) and (25) or (26) the first is believed to offer the easiest and most trustworthy measurement of g provided the vibrator is so placed that its effect is not too different from that of the aerodynamic forces which excite the mode in flutter. Since the summation in Eq. (23) is required for the determination of m_{ii} this method involves only one additional observation for each mode, that of $|a_i|$ or A_e at resonance. Further-

more, it is the product $m\Omega g$ which is of particular interest in flutter analysis, so that this observation combined with frequency data is directly applicable and considerable error in m_{ii} can be tolerated.

Structural Coupling Parameters

Eq. (5) provides a means of determining the structural coupling parameters $\bar{\Omega}_{ij}$ $(i \neq j)$ provided the F functions are known. Physically the F function signifies the force transmitted by the structure to each element of mass as a result of the relative motion of all other elements. The values of the set of vectors F_i are equal to the negative of the set of external force vectors required to produce unit sinusoidal motion in the ith mode alone if the structure were deprived of its inertia. This concept provides a simple means for calculating or estimating the magnitude and distribution of the F's.

It is instructive to consider conditions for symmetry in the structural parameters $\bar{\Omega}_{ij}$. By Eq. (5) symmetry is expressed by the relationship

$$\sum_{\Delta m} F_i f_j \Delta m = \sum_{\Delta m} F_j f_i \Delta m \tag{27}$$

With the assumption of linearity in the structural forces Eq. (27) can be proved as follows. The condition of linearity can be expressed analytically in the form

$$F_i \Delta m_p = \sum_q u_{pq}(f_{iq} - f_{ip}) \tag{28}$$

where the subscripts p and q refer to particular elements. Likewise

$$F_j \Delta m_p = \sum_q u_{pq}(f_{jq} - f_{jp})$$

Hence

$$\sum_p [f_{jp}F_i - f_{ip}F_j]\,\Delta m_p = \sum_p \sum_q [u_{pq}(f_{jp}f_{iq} - f_{ip}f_{jq})] \tag{29}$$

If each term in the summation of Eq. (28) represents a force acting *between* the elements Δm_p and Δm_q it follows that $u_{pq} = u_{qp}$, the double sum in Eq. (29) is equal to zero, and Eq. (27) is therefore satisfied. This assumption of mutual interaction is met in all commonly encountered types of structures and mechanisms.

In the case of non-linear forces extension of the above arguments to "effective" oscillatory forces shows that assymmetry in the $\bar{\Omega}$'s depends upon the relative amplitudes of the coupled degrees of freedom. Where "snubbing" devices are used, whether of the displacement, velocity or acceleration types, it is usually possible to find a pair of degrees of freedom for which the effective $\bar{\Omega}$'s are definitely assymetric. Such problems probably are more easily analyzed by choosing coordinates in which the non-diagonal $\bar{\Omega}$'s vanish.

As in the case of the diagonal structural terms it is convenient to write

$$\bar{\Omega}_{ij} = \Omega_{ij}(1 + g_{ij}\sqrt{-1}), \quad (i \neq j) \tag{30}$$

No generally useful method has been devised for evaluating the frictional coupling term g_{ij} although its existence is easily observable in vibration tests where, at resonance, all parts of the structure do not move in phase. Unlike the diagonal g's, g_{ij}, $(i \neq j)$, may be either positive or negative, but in moderately damped structures it is not likely to be important. It does not contribute to structural energy dissipation but may have an influence on the energy drawn from the airstream. In simple cases of two dimensions and two degrees of freedom, it has been noticed that negative values tend to prevent flutter and positive values tend to promote it, but no case has been found where it cannot be neglected. This condition, of course, depends on the system of coordinates used.

The direct calculation of Ω_{ij} by means of Eq. (5) usually can be carried out without difficulty since only the real part of F_j is involved, and it is equal to the negative of the set of static external forces required to produce the jth deflection mode alone. In some cases it may be desirable to specify a degree of freedom by assuming a particular F and to determine either experimentally or by analysis the corresponding f to be used as the unit coordinate. In many cases, however, shorter methods are possible, as the following development will show.

Let f_1 and f_2 describe any pair of deflection modes of an airfoil which involve bending and twisting only. Further, let

$$\begin{aligned} \int F_2\sigma dx &= G_2 \quad \int F_2 x\sigma dx = x_2 G_2 \\ \int f_2\sigma dx &= w_2 \quad \int f_2 x\sigma dx = p_2 w_2 \end{aligned} \tag{31}$$

where σ is the surface density and the integration extends over the chord; p_2 so defined is the x-coordinate of the center of percussion, and x_2 is that of the load line, both determined for the node of f_2. From Eqs. (9) and (31)

$$\begin{aligned} \int f_1 F_2\sigma dx &= G_2(h_1 + x_2\alpha_1/b_0) = G_2\alpha_1(x_2 - n_1)/b_0 \\ \int f_1 f_2\sigma dx &= w_2(h_1 + p_2\alpha_1/b_0) = w_2\alpha_1(p_2 - n_1)/b_0 \end{aligned}$$

where n_1 is the x-coordinate of the node of mode 1. Substitution in Eq. (5) yields

$$\Omega_{12} = \frac{\int G_2\alpha_1(x_2 - n_1)dy}{\omega_0^2 \int w_2\alpha_1(p_2 - n_1)dy} \tag{32}$$

the integration extending over the span. Similarly,

$$\Omega_{22} = \frac{\int G_2\alpha_2(x_2 - n_2)dy}{\omega_0^2 \int w_2\alpha_2(p_2 - n_2)dy} \tag{33}$$

Hence,

$$\frac{\Omega_{12}}{\Omega_{22}} = \frac{\int G_2\alpha_1(x_2 - n_1)dy}{\int G_2\alpha_2(x_2 - n_2)dy} \times \frac{\int w_2\alpha_2(p_2 - n_2)dy}{\int w_2\alpha_1(p_2 - n_1)dy} \tag{34}$$

In two dimensions this becomes simply

$$\frac{\Omega_{12}}{\Omega_{22}} = \frac{x_2 - n_1}{x_2 - n_2} \times \frac{p_2 - n_2}{p_2 - n_1} \tag{35}$$

Eq. (35) is useful for rough estimates of the ratio Ω_{12}/Ω_{22}. More accurate values can be obtained by estimating the mean values of the integrands in Eq. (34). Actual integration is seldom necessary.

If either one of the modes involves no rotation about a spanwise axis, the corresponding n becomes infinite and the simplification is obvious. If n_2 is infinite, the line p_2 becomes the line of centers of gravity and x_2 the load line for no twist. Only when the latter is straight is it independent of the form of f_2. Then it is commonly referred to as the "elastic axis."

A convenient coordinate system for cantilever airfoils identifies f_1 with twisting about the quarter-chord axis and f_2 with pure bending. In this case Eq. (34) becomes

$$\frac{\Omega_{12}}{\Omega_{22}} = \frac{\int G_2 \alpha_1 x_2 dy}{\int G_2 h_2 dy} \times \frac{\int w_2 h_2 dy}{\int w_2 \alpha_1 x_0 dy} \tag{36}$$

and Eq. (35) becomes

$$\Omega_{12}/\Omega_{22} = x_e/x_0 \tag{37}$$

where x_e is the x-coordinate of the elastic axis.

Generalized Coordinates

The wide variety of flutter problems encountered in aircraft make it impractical at this stage to specify coordinates for all cases. It is for this reason that no restrictions have been placed on the coordinate system in the foregoing discussion. Hence the analyst is completely free to choose any set of coordinates he wishes which will describe the actual motion with sufficient accuracy. Since the amount of labor involved increases rapidly with the number of degrees of freedom, it is desirable to keep this number at a minimum. The coordinate system is so defined that motion associated with a particular coordinate is assumed to be in phase. Hence an essential consideration in determining the minimum number of degrees of freedom is the phase relationship between various parts of the structure. A second consideration is uncertainty in the accuracy of the assumed modes or configurations. For example, if it is not possible to estimate with sufficient accuracy the configuration of a wing in bending as it goes through the flutter cycle, several different configurations may be assumed as separate degrees of freedom. Once these are assumed the analysis automatically determines the relative amplitude and phase which most nearly represent the actual motion.

On the other hand, experience shows that assumed modes known to differ considerably from the actual configurations often lead to surprisingly accurate results. The success of the two-dimensional method of analysis illustrates this point. The use of resonant frequency data on the actual structure is largely responsible for this success. The aerodynamic and inertial parameters are little affected by the character of the assumed modes of motion after they are reduced to a common basis of normality (by applying factors to the rows and columns of an nth-order determinantal equation $2n - 1$ of the elements can be reduced to predetermined magnitudes). Hence, the experienced analyst is not unduly concerned about the accuracy of his coordinate system provided allowance has been made for sufficient phase variation.

Some degrees of freedom which have been found useful in analyses are: (1) pitching of the airplane as a whole about its center of gravity; (2) fuselage vertical bending with rotation of the tail about a lateral axis forward of the stabilizer, sometimes combined with opposite rotation of the wing about a lateral axis near its center of gravity when aerodynamic wing-tail interaction is to be taken into account; (3) rotation of the tail about a vertical axis several chord lengths forward of the stabilizer; (4) rotation of the tail about a longitudinal axis located at either the fuselage center line or the observed node in resonance tests; (5) stabilizer torsion without elevator torsion, the rate of twist being constant; (6) wing bending with constant curvature from root to tip with a node in the plane of symmetry or at a wing station corresponding to the natural node; (7) wing bending with constant curvature from nacelle to tip with a node at the nacelle; (8) wing motion from nacelle to tip with a node running in a curve from the engine center of gravity to a point aft of the tip; (9) wing torsion with constant rate of twist from root to tip with a node at the quarter chord; (10) vertical motion of the wing as a whole; (11) stabilizer bending with constant curvature with a node at the plane of symmetry and outboard vertical surfaces undeformed; (12) the same with nodes at the junctions of vertical and horizontal surfaces; (13) lateral translation of the tail when supported by twin booms; (14) control surface flapping with and without leading or lagging trim tabs; (15) control surface twisting; (16) tab flapping; and (17) rotation of two-dimensional airfoils about arbitrary spanwise axes.

Conclusions

The foregoing development is an attempt to set up well established principles of classical mechanics in a form convenient for numerical work in flutter analysis. Considerable simplification results from the use of the complex notation. Although no additions are made to the existing theory of structures or of aerodynamics, a definite effort has been made to present the subject in such a way that extensions to our limited knowledge can be easily applied when available. It was the aim of the writer to keep the development in a general form in order to cover as many as possible of the problems on aircraft flutter that may arise.

A subsequent paper will present the details involved in the calculation of the various parameters (such as A_{ij} and M_{ij}) and in the solution of the stability equation, Eq. (7). The method of analysis presented in this paper and the calculation schemes to be given later have been used successfully during the past two years on a variety of problems concerning existing airplanes and airplanes in the design stage.

References

[1] Bollay, William, and Brown, Charles D., *Some Experiments on Wing Flutter*, Journal of the Aeronautical Sciences, Vol. 8, No. 8, pages 313–318, June, 1941.

[2] *Tacoma Narrows Bridge* (Abstract), Mechanical Engineering, Vol. 63, No. 7, page 545, July, 1941.

[3] Theodorsen, Th., *General Theory of Aerodynamic Instability and the Mechanism of Flutter*, N.A.C.A. Technical Report No. 496, 1935.

[4] Silverstein, A., and Joyner, Upshur T., *Experimental Verification of the Theory of Oscillating Airfoils*, N.A.C.A. Technical Report No. 673, 1939.

[5] Reid, Elliott G., and Vincenti, Walter, *An Experimental Determination of the Lift of an Oscillating Airfoil*, Journal of the Aeronautical Sciences, Vol. 8, No. 1, pages 1–6, November, 1940.

[6] Civil Aeronautics Manual 04, *Airplane Airworthiness*, pages 3–25, February 1, 1941.

[7] Frazer, R. A., Duncan, W. J., and Collar, A. R., *Elementary Matrices*, Cambridge University Press, 1938.

[8] Loring, S. J., *General Approach to the Flutter Problem*, S.A.E. Journal, Vol. 49, No. 2, pages 345–356, August, 1941.

[9] Theodorsen, Th., and Garrick, I. E., *Mechanism of Flutter*, N.A.C.A. Technical Report No. 685, 1940.

[10] Burgess, C. P., *Frequencies of Cantilever Wings in Beam and Torsional Vibration*, N.A.C.A. Technical Note No. 746, 1940.

[11] Coleman, Robert P., *Damping Formulas and Experimental Values of Damping in Flutter Models*, N.A.C.A. Technical Note No. 751, 1940.

On the Reaction of an Elastic Wing to Vertical Gusts

WILLIAM R. SEARS AND BRIAN O. SPARKS

Northrop Aircraft, Inc., and Bell Aircraft Corporation

Introduction

THE PROBLEM of the behavior of an elastic wing during and subsequent to its entrance into a vertical gust has been considered by several authors,[1, 2, 3] who have made various assumptions regarding the properties of the wing and the nature of the aerodynamic forces. These forces have usually been calculated by neglecting entirely the "non-stationary flow" effects or by including them in certain terms and neglecting them in others. The results have often shown that wing deflections (and therefore stresses) considerably greater than those corresponding to steady-state values are produced by certain combinations of gust gradient and wing elastic properties.

The present paper is a step in an attempt to determine whether this conclusion may be due in part to the neglect of non-stationary effects.

For this purpose the case of a wing elastic in bending but perfectly rigid in torsion is considered. It is treated approximately by assuming two-dimensional flow conditions at a typical section of the wing and representing the elastic properties of the wing by a spring restraining the vertical motion of this section. The aerodynamic forces are then calculated from the theory of two-dimensional thin airfoils in non-uniform motion. The use of this theory permits proper account to be taken of the "lag" of both the lift due to the gust and the lift due to the vertical motion of the wing.

The Equation of Motion

The equation of motion for the wing section under consideration is

$$m\ddot{z} + kz = L \tag{1}$$

where

- m = mass of wing, including the additional apparent mass of air in vertical motion, per unit span.
- z = upward deflection of the wing.
- k = spring constant representing the bending stiffness of the wing, i.e., restoring force on the section considered per unit upward deflection.
- L = instantaneous total lift per unit of span.

and where dots indicate differentiation with respect to the time, t.

Received September 16, 1941.

A method has been suggested[4] to calculate the lift L_g on a rigid wing entering a vertical gust distribution $w(s)$, where $s = \bar{U}t$ = distance traveled by the wing, in half-chords. Using the "superposition integral," this lift can be expressed as

$$L_g(s) = \pi\rho U c \int_0^s w(\sigma)\Psi'(s - \sigma)d\sigma \tag{2}$$

where

- ρ = air density.
- U = velocity of flight (ft per sec.) = $\bar{U}c/2$.
- $\bar{U}$ = velocity of flight in half-chords per sec.
- c = wing chord (ft.).
- $\Psi(s)$ = a function calculated by von Kármán and Sears giving the lift on a rigid airfoil entering a sharp-edged gust, s being measured from the instant the leading edge begins to enter the gust.

Since the wing is not rigid in the present case, there must be added to L_g the lift due to the vertical velocity of the wing. Again using the "superposition integral,"* this is found to be

$$L_v(s) = \pi\rho U c \int_0^s (d\dot{z}(\sigma)/d\sigma)[1 - \Phi(s - \sigma)]d\sigma \tag{3}$$

where $1 - \Phi(s)$ is Wagner's function,[4] which gives the lift on an airfoil following a sudden change of its angle of attack at $s = 0$.

It is convenient to use s as the independent variable in Eq. (1). Then, writing $L = L_g + L_v$,

$$m\bar{U}^2 z'' + kz = L_g + L_v \tag{4}$$

where the primes represent differentiation with respect to s.

This equation, which in accordance with Eqs. (2) and (3), is actually an integro-differential equation, is to be solved for $z(s)$ with the initial conditions $z(0) = \dot{z}(0) = 0$ for a given gust profile $w(s)$.

The Equation of Motion in Operational Form

This problem is most conveniently solved by means of Heaviside's operational methods. The notation used here is that used by Pipes,[5] except that the independent variable will be denoted by s instead of t. If a function $f(s)$ satisfies certain existence and continuity conditions on itself and its first derivatives, it may be represented by the complex integral

* Reference 4, Eq. (42).

$$f(s) = (1/2\pi i)\int_{a-i\infty}^{a+i\infty} F(p)e^{ps}dp/p \qquad (5)$$

where $F(p) = p\int_{-\infty}^{\infty} f(s)\, e^{-ps}dt$

and a is a real number great enough so that all singularities of $F(p)/p$ occur for $R(p) < a$. The function $F(p)$ is called the direct Laplacian Transform or *image* of $f(s)$, and the relationship between $f(s)$ and $F(p)$ is denoted by writing $F(p) \doteqdot f(s)$, after the notation of B. van der Pol. A few of the more useful theorems and transforms are given here without proof to show the methods of transforming the integro-differential equation into operational form.

Theorem I

If $g(p) \doteqdot h(s)$, then

$$p^n g(p) - \sum_{k=0}^{n-1}\left(\frac{d^k h}{ds^k}\right)_{s=0} p^{n-k} \doteqdot \frac{d^n h(s)}{ds^n}$$

Theorem II

If $g_1(p) \doteqdot h_1(s)$ and $g_2(p) \doteqdot h_2(s)$, then

$$g_1(p)g_2(p)/p \doteqdot \int_0^s h_1(u)\, h_2(s-u)du$$

Elementary Transforms

If $h(s) = 1(s) = \left.\begin{matrix} 1 \text{ for } s \geqq 0 \\ 0 \text{ for } s < 0 \end{matrix}\right\}$, then $1 \doteqdot h(s)$.

If $h(s) = e^{-\alpha s}$, then $p/(p+\alpha) \doteqdot h(s)$.

If $h(s) = (1 - e^{-\alpha s})$, then $\alpha/(p+\alpha) \doteqdot h(s)$.

Each term of Eq. (4) can now be put into operational form, as follows:

(1) By use of Theorem I, assuming that $z(s) = 0$ for $s \leqq 0$, the first term can be written as

$$m\overline{U}^2p^2h(p) \doteqdot m\overline{U}^2z''(s)$$

where $h(p) \doteqdot z(s)$.

(2) By use of Theorems I and II, from Eq. (2), noting that $\Psi(0) = 0$, L_g becomes

$$\pi\rho\overline{U}^2(c/2)^2cg(p)\psi(p) \doteqdot L_g(s)$$

where $g(p) \doteqdot w(s)/U$ and $\psi(p) \doteqdot \Psi(s)$.

(3) By use of Theorems I and II, from Eq. (3), noting that $\overline{U}ph(p) \doteqdot \dot{z}(s) = \overline{U}z'(s)$, L_v becomes

$$-\pi\rho\overline{U}^2(c^2/2)ph(p)[1 - \varphi(p)] \doteqdot L_v(s)$$

where $\varphi(p) \doteqdot \Phi(s)$.

Since equality of two functions implies equality of their images, the equation of motion can now be written in operational form:

$$\{m\overline{U}^2p^2 + k + \pi\rho\overline{U}^2(c^2/2)p[1 - \varphi(p)]\}h(p) = \pi\rho\overline{U}^2(c/2)^2cg(p)\psi(p) \qquad (6)$$

or

$$h(p) = \frac{B\psi(p)}{p^2 + A + Bp[1 - \varphi(p)]}(c/2)g(p) \doteqdot z(s) \qquad (7)$$

where $A = k/m\overline{U}^2$ and $B = \pi\rho c^2/2m$.

The parameter A may be called the "dimensionless stiffness," while B is twice the ratio of the additional apparent air mass to the total mass m, and may be considered as the dimensionless mass parameter. A is proportional to the square of the ratio between the natural frequency of the wing in bending and the velocity in half-chords per second; in flutter calculations this ratio is often called the "reduced" natural frequency of the wing in bending.

Approximations to the Lift Functions

The calculation of $z(s)$ for various gust functions $g(p) \doteqdot w(s)$ can now be carried out if $\psi(p)$ and $\varphi(p)$ are known. Sears[6] gives these operators in terms of certain Bessel functions which are practically intractable in the present problem. However, an approximation to Wagner's function $1 - \Phi(s)$ has been suggested by Jones,[7] having a particularly simple image:

$$1 - \Phi(s) \cong 1 - a_1e^{-\lambda_1 s} - a_2e^{-\lambda_2 s} \qquad (8)$$

for which

$$1 - \varphi(p) = 1 - [a_1p/(p+\lambda_1)] - [a_2p/(p+\lambda_2)]$$

where $a_1 = 0.165$, $a_2 = 0.335$, $\lambda_1 = 0.0455$, and $\lambda_2 = 0.300$.

This suggests the possibility of a similar approximation to the function $\Psi(s)$:

$$\Psi(s) \cong 1 - b_1e^{-\mu_1 s} - b_2e^{-\mu_2 s} \qquad (9)$$

for which

$$\psi(p) = 1 - [b_1p/(p+\mu_1)] - [b_2p/(p+\mu_2)]$$

It is found by trial that the following numerical values provide the best approximation:*

$$b_1 = b_2 = 1/2,\ \mu_1 = 0.130,\ \mu_2 = 1$$

* It will be seen that the approximate form of $\Psi(s)$ does not have a vertical tangent at $s = 0$ as does the exact function. This is not expected to have a great effect on the accuracy of the results obtained.

Using the forms of φ and ψ given in Eqs. (8) and (9), Eq. (7) becomes

$$h(p) = B\frac{(p+\mu_1)(p+\mu_2) - b_1p(p+\mu_2) - b_2p(p+\mu_1)}{(p+\mu_1)(p+\mu_2)} \times \frac{(p+\lambda_1)(p+\lambda_2)}{(p^2+Bp+A)(p+\lambda_1)(p+\lambda_2) - Bp^2[a_1(p+\lambda_2) + a_2(p+\lambda_1)]}(c/2)g(p) \doteqdot z(s) \qquad (10)$$

If the final value of $w(s)$ is $w(\infty)$, the final steady-state deflection will be $z(\infty) = \pi\rho U w(\infty)c/k = (B/A) \times (c/2)w(\infty)/U$. Hence Eq. (10) can be used to determine the dimensionless deflection $z(s)/z(\infty) = z^*(s)$, say, which depends only on the two dimensionless parameters A and B.

Evaluation of the Operator

The operator $h(p)$ in Eq. (10) can be evaluated by application of "Heaviside's Expansion Theorem"[5]: For operators of the type under consideration

$$z(s) = (1/2\pi i)\int_{a-i\infty}^{a+i\infty}(e^{ps}h(p)/p)dp = \sum \text{(residues of } (e^{ps}h(p)/p) \text{ in the } p \text{ plane)}$$

$$= [N(0)/M(0)] + \sum_{r=1}^{n}[N(p_r)e^{p_r s}/p_r M'(p_r)] \qquad (11)$$

where $h(p) = N(p)/M(p)$, $N(p)$ and $M(p)$ are polynomials in p and the order of $M(p)$ is at least as high as that of $N(p)$, and the polynomial $M(p)$ has the n distinct zeros $p = p_1, p_2, \ldots, p_n$. Hence, assuming that $g(p)$ is given in convenient form, the evaluation of $h(p)$ in Eq. (10) depends only on the determination of the zeros of the denominator. These occur when $p = -\mu_1, -\mu_2$, and the four roots of

$$p^4 + \alpha p^3 + \beta p^2 + \gamma p + \delta = 0 \qquad (12)$$

where

$$\alpha = \lambda_1 + \lambda_2 + B(1 - a_1 - a_2) = 0.3455 + B/2$$
$$\beta = A + B\lambda_1(1 - a_2) + B\lambda_2(1 - a_1) + \lambda_1\lambda_2$$
$$= A + 0.2807B + 0.01365$$
$$\gamma = B\lambda_1\lambda_2 + A(\lambda_1 + \lambda_2) = 0.01365B + 0.3455A$$
$$\delta = A\lambda_1\lambda_2 = 0.01365A$$

Scope of the Present Investigation

The wing deflection, which is proportional to the bending stress in the wing structure, is calculated here in dimensionless form for two gust profiles:

(1) sharp-edged gust: $w(s)/U = 1(s) = \begin{cases} 0 \text{ for } s < 0 \\ 1 \text{ for } s \geqq 0 \end{cases}$

for which $g(p) = 1$.

(2) graded gust: $w(s)/U = \begin{cases} 0 \text{ for } s < 0 \\ 1 - e^{-as} \text{ for } s \geqq 0 \end{cases}$ for which $g(p) = a/(p + a)$.

The value taken here for a is 0.75, which corresponds to the gust profile drawn in Fig. 2. This is a gust which reaches 90 per cent of its final strength about 3 half-chords from its edge.

For these two cases the calculations of z^* have been carried out for $B = 2/7$ and $A = 1.355$, 0.0845 and 0.0375. The value $B = 2/7$ has been chosen arbitrarily to represent a class of airplane wings. It corresponds to a wing weight of $0.42c$ lbs. per sq.ft. at sea-level standard conditions, or to lighter wings at higher altitudes.

In these calculations Horner's method was employed to determine the real roots of the quartic (Eq. (12)). Two real and two complex roots were found in each of the cases considered; the complex roots were easily calculated from the quadratic equation remaining after the real roots were located.

The results of these calculations are presented in Figs. 1 and 2, where z^* is plotted against the dimensionless time variable $t^* = t\sqrt{k/m} = s\sqrt{A}$ for the four values of A. The variable t^* is 2π times the ratio of t to the natural period of vibration of the wing, $2\pi\sqrt{m/k}$, where t is measured from the instant that the leading edge begins to enter the gust.

In Figs. 1 and 2 it is seen that the principal effect of increasing the dimensionless stiffness is to increase the tendency of the wing to oscillate after it strikes the gust. In several cases the oscillation carries the deflection slightly beyond the steady-state asymptotic value.

If the curves of Figs. 1 and 2 are compared, the effect of grading the gust is seen to be small in the cases investigated. For $A = 1.355$ and 0.338 the deflections increase more slowly and the amplitudes of the oscillations are diminished. For $A = 0.0845$ and 0.0375 the effects of grading the gust are negligible.

Numerical Example

As a numerical example, the following properties are assumed for the wing:

$c = 7.5$ ft.
$m = 0.7354$ slugs per ft. span.
$k = 622.5$ lbs. per ft. per ft. span.

These values (to which the value $B = 2/7$ corresponds) have been used in a thesis by A. E. Lombard, Jr.,[8] to represent typical values for modern airplane wing construction.† Using these numerical values the dimensionless values of Figs. 1 and 2 can be interpreted in dimensional form. The flying speeds corresponding to the four values of A, and the steady-state deflections $z(\infty)$ due to a gust of 1 ft. per sec. final intensity at sea-level standard conditions are as follows:

A	U (ft. per sec.)	$z(\infty)$ for $w(\infty) = 1$ ft. per sec. (ft.)
1.355	93.75	0.0084
0.338	187.5	0.0169
0.0845	375.0	0.0338
0.0375	562.5	0.0507

The deflections for different gust intensities are directly proportional to $w(\infty)$.

† Lombard expresses the same values as follows:
(wing mass)/(additional apparent air mass) = 6.0 at sea level.
Natural frequency in bending = $\sqrt{k/(\text{wing mass})} = 10\pi$ radians per sec.
= 5 cycles per sec.

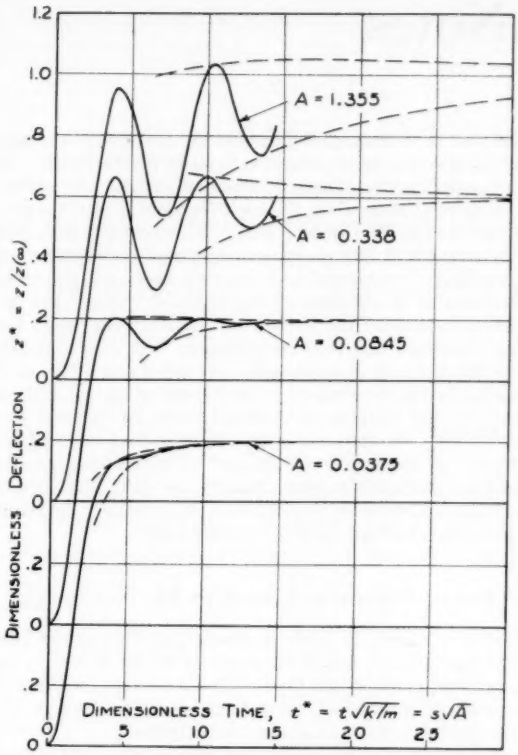

FIG. 1. Dimensionless deflection due to a sharp-edged gust, for various values of the dimensionless stiffness parameter A. The value 2/7 has been assumed for the mass parameter B. (Note that the origin of the z^* scale has been shifted for each value of A.)

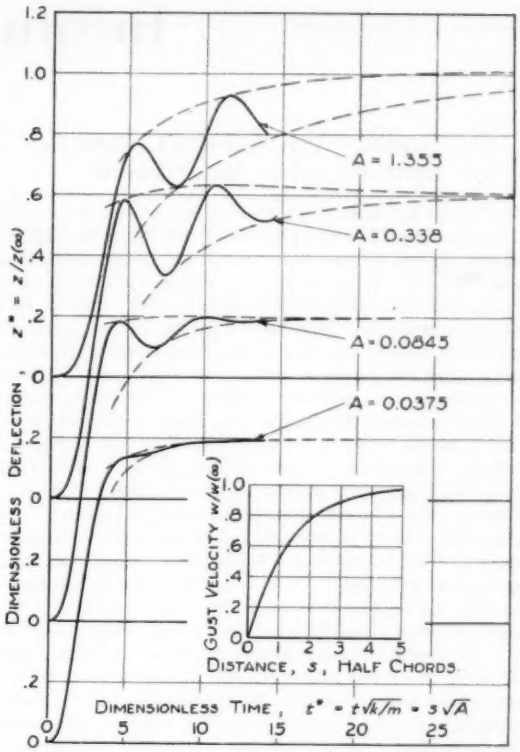

FIG. 2. Dimensionless deflection due to an exponentially graded gust, for various values of the dimensionless stiffness parameter A. The value 2/7 has been assumed for the mass parameter B. The inset graph show the gust profile assumed.

On this basis it is seen that the cases that produced the greatest dimensionless deflections ($A = 1.355$ and 0.338) actually correspond to low speeds of flight and hence are not critical. In other words, the fortunate circumstance arises that the aerodynamic forces damp out the oscillation at high flying speeds, so that stresses greater than the steady-state values do not occur at high speeds.

CONCLUSIONS

It is concluded from the results presented here that inclusion of all of the non-stationary aerodynamic effects in the calculation leads to relatively low rates of wing deflection and maximum deflections only slightly greater than the asymptotic values. The large deflections calculated in certain cases by other approximate theories do not appear in the particular cases considered here.

These conclusions are strictly applicable only to the cases of infinite torsional rigidity considered here. In application to actual airplane wings entering gusts the calculations should be extended to account for torsional flexibility. The wing deflection will then depend intimately on the relative rigidities in bending and torsion and on the location of the elastic and inertial axes. The results presented here can be expected to indicate the behavior of wings that are relatively very stiff in torsion.

REFERENCES

[1] Küssner, H. G., *Beanspruchung von Flugzeugflügeln durch Böen*, Zeitschrift für Flugtechnik und Motorluftschiffahrt, Vol. 22, page 579, 1931. (Translated as N.A.C.A. Technical Memorandum No. 654, 1932.)

[2] Bryant, L. W., and Jones, I. M. W., *Stressing of Aeroplane Wings Due to Symmetrical Gusts*, A.R.C. R. & M. No. 1690, 1936.

[3] Minelli and Gröbner, *Indagini sulle vibrazioni dei velivoli (Vibrazioni alari prodotte da una raffica verticale)*, l'Aerotecnica, Vol. 19, page 373, 1939.

[4] von Kármán, Th., and Sears, W. R., *Airfoil Theory for Non-Uniform Motion*, Journal of the Aeronautical Sciences, Vol. 5, No. 10, page 379, August, 1938.

[5] Pipes, L. A., *The Operational Calculus*, Journal of Applied Physics, Vol. 10, pages 172–180, 258–264, 301–312, 1939.

[6] Sears, W. R., *Operational Methods in the Theory of Airfoils in Non-Uniform Motion*, Journal of the Franklin Institute, Vol. 230, page 95, 1940.

[7] Jones, Robert T., *Operational Treatment of the Non-Uniform Lift Theory in Airplane Dynamics*, N.A.C.A. Technical Note No. 667, 1938.

[8] Lombard, Albert E., Jr., *An Investigation of the Conditions for the Occurrence of Flutter in Aircraft, and, the Development of Criteria for the Prediction and Elimination of Such Flutter*, Thesis, California Institute of Technology, 1938.

Institute Notes

Dr. Theodore von Kármán Chosen for Sylvanus Albert Reed Award

The Fellows and Honorary Fellows of the Institute have chosen Dr. Theodore von Kármán, Director of the Daniel Guggenheim Graduate School of Aeronautics and the Guggenheim Aeronautical Laboratory, California Institute of Technology, to receive the Sylvanus Albert Reed Award for 1941. This honor is conferred annually in recognition of a notable contribution to the aeronautical sciences resulting from experimental or theoretical investigations, the beneficial influence of which on the development of practical aeronautics is apparent. With the citation "for the development of a satisfactory theory of the influence of curvature on the buckling characteristics of aircraft structures," it will be presented to Dr. von Kármán at the I.Ae.S. Tenth Annual Meeting. He is an Honorary Fellow of the Institute.

Theodore von Kármán's accomplishments in a career of over thirty years devoted to research and teaching are unparalleled as a total contribution to the fundamental sciences on which modern aviation is based. A native of Budapest, he graduated from that city's Royal Technical University in 1902 as a Mechanical Engineer. In 1908 he received a Ph.D. from the University of Göttingen, Germany, and remained on the faculty there as Lecturer in Applied Mechanics and Aerodynamics. In 1913 he was appointed Director of the Aeronautical Institute of Aachen University and held this post until 1929, together with assignments to various other duties during this period. From 1915 to 1917 he served as head of a research department of the Austro-Hungarian Army Air Corps where he carried on work in helicopter development. He first visited the United States in 1926 at the invitation of the Guggenheim Fund for the Promotion of Aeronautics, where he lectured at several universities and research institutions. The following year was spent in giving lectures at the Universities of Tokyo, Fukuoka, Nanking and Calcutta.

In 1928 and 1929 Dr. von Kármán divided his time between the University of Aachen and California Institute of Technology. Since 1930 he has been Director of the Guggenheim Aeronautical Laboratory and the Daniel Guggenheim Graduate School of Aeronautics at Cal Tech.

A large part of his work has been concerned with fluid flow and aerodynamics. His classical paper of 1912 presented the "Kármán Vortex Street" conception of the stable arrangement of vortices explaining the form drag of bluff bodies. In 1921 his study on boundary layer phenomena introduced the famous "Kármán Integral Relation" and served as the starting point for other investigations in this field. His theory of "Mechanical Similarity and Turbulence" led to the first rational and explicit expression for skin friction of smooth surfaces which has had wide practical application in airplane design and naval architecture. In recent years he made valuable contributions to the theory of compressible fluids, and supersonic flow.

In connection with aerodynamics as applied to aircraft, he produced a fundamental work with Trefftz on longitudinal stability of airplanes, the theory of the so-called Kármán-Trefftz airfoil sections, studies on potential flow around airfoils of arbitrary section, helicopter theory, soaring flight, pressure distribution on airship hulls, wind tunnel interference, and loads on seaplane floats.

He made contributions in the field of elasticity and structures, to which his citation for the Reed Award refers, beginning with his first paper published after graduation from the Technical University in Hungary. It dealt with the buckling of struts. His early training and experience as a design engineer has manifested itself in his feeling for the needs and problems of the practical engineer to a degree unusual in the theoretical scientist. He has published papers on the calculation of strength and stiffness of cantilever airplane wings, the basic theory of beams, the processes involved in sheet metal rolling. His recent and basic work on the strength of thin sheets in compression involved tests on the buckling of cylindrical and spherical shells and led to the formulation of a non-linear, large-deflection theory—the first adequate method for calculating the ultimate compressive load which a stiffened thin sheet can support. It is in almost daily use in the design of monocoque aircraft structures. This study was published in three papers in the Journal of the Aeronautical Sciences—"The Buckling of Spherical Shells by External Pressure" (1939), "The Influence of Curvature on the Buckling Characteristics of Structures" (1940), and "The Buckling of Thin Cylindrical Shells Under Axial Compression" (1941). The technical publications by Dr. von Kármán on aeronautics and other subjects number altogether about seventy papers.

Octave Chanute Award to M. N. Gough

Melvin N. Gough, A.F.I.Ae.S., Senior Test Pilot at the Langley Memorial Aeronautical Laboratories of the N.A.C.A., has been selected to receive the Octave Chanute Award for 1941 "for his outstanding contributions to fundamental research in aeronautics as conducted on airplanes in actual flight."

Immediately after his graduation with a B.S. in M.E. from Johns Hopkins University in 1926, he was employed by the N.A.C.A. as a Junior Mechanical Engineer in the Propeller Research Section of the laboratory at Langley Field for two years. Then he took the Naval Pilot Training course, obtaining a commission as Lieutenant in the U.S. Naval Reserve, which he still holds. On his return to the N.A.C.A. in 1929, he was transferred to his present work in the Flight Research Section as a Pilot Engineer. He has served as a consulting test pilot for short periods with Brewster Aeronautical Corp., Fleetwings, Inc., and other aircraft manufacturers.

Mr. Gough's combined ability as an engineer and test pilot has enabled him to contribute much to an understanding of the problems of both. Many of his technical reports are included in N.A.C.A. publications and papers presented before Institute and other aeronautical meetings. They cover such subjects as studies to improve stalling characteristics, stability, handling characteristics, flying qualities and other factors leading to improvement in the safety of modern airplanes. His research on the field of view of the pilot, spinning, maneuverability and flow-force limitations have been of great value to military airplane designers.

The Octave Chanute Award is awarded each year to a pilot chosen by a committee consisting of the Chief of the Army Corps, Chief of the Navy Bureau of Aeronautics, Director of the National Bureau of Standards, Chairman of the Civil Aeronautics Board, Director of Research of the N.A.C.A., President of the Institute of the Aeronautical Sciences, and Executive Vice-President of the Institute. The previous recipients were Edmund T. Allen and Howard Hughes.

Gifts of Manuals to Library

The Curtiss-Wright Corporation has recently donated to The Paul Kollsman Library six editions of its Instruction Books on various models of the Wright "Whirlwind" and "Cyclone" engines, two overhaul manuals, an Installation Manual, Specifications Tables and a set of Service lectures on Engines. The gift

Tenth Annual Meeting and Honors Night Dinner

Celebrating the Institute's tenth year as this country's only scientific aeronautical society, the Tenth Annual Meeting next month will be the most notable and well attended of any yet held. Such interest has been shown in the technical sessions, for which about seventy papers have been received and approved by session chairmen, that many of the subjects will require two sessions.

Honors Night Dinner

Plans for the Honors Night Dinner are not announced at this time owing to the uncertainty of present conditions. Members will be advised early in January of the decision of the Council regarding the most appropriate way of presenting the honors and awards of the Institute.

Technical Sessions of the Annual Meeting

Pupin Physics Laboratories, Columbia University, New York

The excellent lecture hall facilities of Columbia University will again be the setting for the technical meetings. Luncheon will be served each day at the Columbia University Men's Faculty Club convenient to the lecture hall. The schedule for the various sessions is given below. A tentative program listing the papers to be presented is being sent to all members of the Institute this month and will be published in full in the January issue of the Aeronautical Review Section.

Wednesday, January 28

9:15 a.m. Structures, Part 1, Room 401 — Power Plants, Room 428
2:00 p.m. Structures, Part 2, Room 401 — Radio and Instruments, Room 428
5:00 p.m. Annual Business Meeting, Room 428
8:00 p.m. Design, Room 401

Thursday, January 29

9:15 a.m. Materials, Part 1, Room 401 — Rotating Wing Aircraft, Room 428
2:00 p.m. Materials, Part 2, Room 401 — Physiologic Problems, Part 1, Room 428
8:00 p.m. Physiologic Problems, Part 2, Room 401

Friday, January 30

9:15 a.m. Aerodynamics, Part 1, Room 401 — Meteorology, Part 1, Room 428
2:00 p.m. Aerodynamics, Part 2, Room 401 — Meteorology, Part 2, Room 428
8:00 p.m. Air Transport, Room 401 — Meteorology, Part 3, Room 428

Saturday, January 31

9:15 a.m. Meteorology, Part 4, Room 428

also included a brochure and an Instruction Manual for Curtiss Electric Propellers.

Such instruction and maintenance manuals for aircraft and equipment are very useful additions to the lending and reference libraries. Aircraft companies are urged to send duplicate copies of any manuals like these that they can spare for the use of Institute members at the Pacific Aeronautical Library in Hollywood and The Paul Kollsman Library in New York.

Pacific Aeronautical Library Open During Evenings

The Pacific Aeronautical Library, established by the Institute on October 1 at 6715 Hollywood Boulevard in Hollywood, has already become such a useful information and study center for the thousands of technical men engaged in the aviation industry in the area that evening hours have been arranged to satisfy

The Outpost Building, at 6715 Hollywood Boulevard, Hollywood, California, in which the Pacific Aeronautical Library is housed.

the many requests for this service. The Library is now open to visitors at the following hours:

Mondays—9:00 a.m. to 5:00 p.m.
Tuesdays through Fridays—9:00 a.m. to 9:00 p.m.
Saturdays—9:00 a.m. to 12:00 noon.

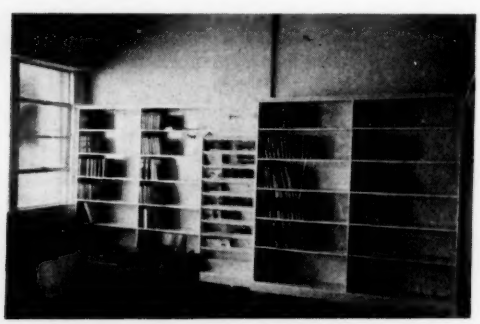

An interior view of the Library.

There are over 1000 books already available in the Library's collection, furnished by the Institute through the Paul Kollsman Fund. Current and back issues of many aeronautical periodicals are also on file.

The Library has received 8000 catalog cards from the Library of Congress to be made into a union catalog of books available in the Los Angeles area. These also form an excellent check list of all books published on aeronautical subjects.

Readers may keep up to date on the latest material in the field by reviewing the books on the Current Book Shelf to which all new volumes are added as soon as released by the publishers.

Since the Pacific Aeronautical Library is supported by aircraft companies on the West Coast, it is maintained as a free service to readers. Members of the Institute and others living in or near Los Angeles who may have aeronautical books which they would be willing to donate to the new library are requested to get in touch with E. W. Robischon, the Director.

Institute Employees Win Piper Cub Airplane

Seven members of the Institute's staff recently formed a flying club. The only thing they lacked was an airplane. Accordingly, they determined to win one via the Wings of Destiny program which awards a Piper Cub to some lucky person each week.

For almost three months, they submitted entries to the contest. Once they were runner-ups and were given a consolation prize of $10.00. On November 21, they won second prize: a Lear, 3-band, portable radio, and on the following Friday, they finally won the airplane.

The airplane was awarded to Miss Marjorie Rodé, Secretary-Treasurer of the Club over whose signature all the entries were made. William V. Humphrey is President, and James J. Coltiletti is Vice-President. The other members are: William S. Friedman, Joseph M. Fagan, and John F. Hoffman.

News of Institute Members

Walter H. Beech, M.I.Ae.S., has acquired joint control, with Charles G. Yankey, of the Culver Aircraft Corp. of Wichita. He organized and managed the Travelair Manufacturing Co. from 1925 until its merger with the Curtiss-Wright Corp. in 1932, then organized the Beech Aircraft Corporation, of which he is now President.

Fred J. Boll, Technical Member, has been made Manager of the Research Laboratory of Lockheed Aircraft Corp. A graduate of the Lockheed-Cal Tech special course for engineers held last fall, he served as Supervisor of Production Processes, Chemical and Metallurgical Testing, in Lockheed's Research Department until this recent promotion.

Henry H. Budds, M.I.Ae.S., has joined the staff of Ranger Aircraft Engines Division, Fairchild Engine & Airplane Corp., to take charge of quantity production of Ranger in-line air-cooled engines recently commenced. Mr. Budds brings fifteen years of experience with Briggs Manufacturing Corp., where, as General Manager of its Airplane Parts Division for the past eighteen months, he directed this company's rapidly expanding production of airplane components.

Charles H. Chatfield, F.I.Ae.S., formerly Director of Research for United Aircraft Corp., has been made Secretary of the corporation. He has been associated with United in engineering and research capacities since 1929.

Charles Christenson, Technical Member, has left the Engineering Department of Grumman Aircraft Engineering Corp. to take a position as Design Engineer with the Bristol Aircraft Division of Universal Moulded Products Corp. This company recently acquired the assets of Monocoupe Airplane & Engine Corp. of Orlando, Fla., the Bristol Aircraft Corp. of Bristol, Va., and Bristol Aircraft Products Ltd. of Belleville, Ontario, whose plants at these locations it now operates as subsidiaries.

Col. J. Carroll Cone, M.I.Ae.S., Assistant Vice-President of Pan American Airways, has been elected Commander for 1942 of Air Service Post No. 501 of the American Legion. This Post is the largest, oldest and most active of the Air Service Posts of

the Legion. Colonel Cone has been an active American Legion member ever since he joined soon after World War I. His war service included nearly two years in France, where he was Chief Instructor at a French flying school, later Commander of the 3rd Pursuit Group which saw action in the Toul, Argonne and St. Mihiel sectors.

Lt. John J. Crane, Technical Member, a graduate of Wayne University and the U.S. Army Air Corps Advanced Flying School, is now a flying officer with the Caribbean Air Force stationed at the Panama Air Depot.

Charles H. Dolan, A.F.I.Ae.S., has been made General Manager of the recently formed Aviation Division of the Chicago Pneumatic Tool Co. at their factory at Garfield, N. J. For the past year he had been President of the Wissahickon Tool Works, a division of the Empire Ordnance Corp., for which he set up a plant and organization at Bala-Cynwyd, Pa., for the manufacture of gun recoil sets and other armament devices. Mr. Dolan was Vice-President of Intercontinent Corporation from 1936 to 1940 and has been active in aviation since 1914, principally in air transportation after World War I.

Adolph Herzog, M.I.Ae.S., formerly Chief Draftsman for Platt-LePage Aircraft Co., has joined the engineering staff of AGA Aviation Corp. He has been connected with rotating-wing aircraft development and other aeronautical concerns in the Philadelphia region since 1926.

Nicholas Ivanovic, Technical Member, has been promoted from Assistant (P-2) to Associate Aeronautical Engineer (P-3) at the Naval Aircraft Factory in Philadelphia.

Agnew E. Larsen, A.F.I.Ae.S., is now associated with Machine & Tool Designing Co., mechanical and consulting engineers of Philadelphia, engaged in designing production machinery for aircraft and other defense industries. Mr. Larsen is well known in aviation circles for his participation in rotating-wing aircraft development since 1923 with Pitcairn and Cierva in England as well as this country. He was Chief Engineer of the Autogiro Company of America and Vice-President and General Manager of the Pitcairn-Larsen Autogiro Co.

Agne T. Lundgren, M.I.Ae.S., who has been with the Engineering Department of Vega Airplane Co. in the position of Production Engineer for the past year and a half, has been appointed Assistant Night Superintendent of Manufacturing with the same company.

At the meeting of the stockholders of Northrop Aircraft, Inc., held in October, **John K. Northrop,** President, was re-elected a member of the Board of Directors.

E. William Murphy, Technical Member, has been appointed District Maintenance Supervisor for the C.A.A. in Albuquerque, New Mexico. He recently returned from Honduras where he had been a Maintenance Engineer with the airline TACA (Transportes Aereos Centro Americanos).

Nels E. Nylin, Technical Member, is now a Senior Machine Designer at Timm Aircraft Corp. A graduate of M.I.T. with four years' experience in the design of machine and production equipment of various kinds, Mr. Nylin graduated from the Lockheed-Cal Tech aeronautical engineering course last year and served for a time on the Lockheed engineering staff.

Thomas N. Pamplin, Technical Member, who received his B.S. in Engineering from Texas A. & M. last June, is an Apprentice Engineer with Pan American Airways System at Brownsville, Texas.

The name of the Pitcairn-Larsen Autogiro Co. was changed in October to the AGA Aviation Corporation. **Harold F. Pitcairn,** M.I.Ae.S., is one of the Directors. **Fred J. Knack,** A.F.I.Ae.S., will continue as Chief Engineer. He was formerly Chief Engineer of Luscombe Airplane Corp. Other Institute members on the staff of the company are **Paul H. Stanley,** Chief Aerodynamicist, **J. P. Perry,** Chief of Structures, and **John R. Huber,** Structural Analyst.

Dr. Willy Prager, A.F.I.Ae.S., has recently arrived from Turkey to take the post of Professor of Applied Mechanics in the Division of Engineering, Brown University. Dr. Prager had been Professor of Mechanics and Higher Geometry at the University of Istanbul since 1933. He is a former pupil of Ludwig Prandtl and after his graduation from the University of Göttingen, returned there in 1929 to lecture on mechanics, strength of materials and aircraft statics. He was for a time Chief of the Statics Department of the Fieseler Airplane Works.

Bruce R. Prentice, Technical Member, has been made an Engineer in the Aeronautic Equipment Division of the General Electric Company at Schenectady. He has been with General Electric since 1931, when he started in as a Student Engineer after receiving his B.S. in E.E. from Kansas State College.

Boyd E. Quate, Technical Member, Meteorologist for Pan American-Grace Airways, was promoted by the company on September 1 to the position of Sectional Meteorologist (Acting) for Chile.

Scott Rethorst, Technical Member, has joined The Goodyear Tire & Rubber Co. as an Aeronautical Research Engineer. He recently left his position as Chief Process Engineer for Vultee Aircraft, Inc. He is a graduate of M.I.T. in Chemical Engineering and had four years' experience with Columbia Steel Co. in the development of stainless steel for aircraft before going to Vultee.

Dr. Clifford P. Seitz, M.I.Ae.S., has returned to the Department of Psychology, College of the City of New York, where he had previously been an Instructor, after two years in a similar position at the University of Alabama. Dr. Seitz has collaborated with Dr. Ross A. McFarland and others in experimental psychological studies on high altitude effects.

E. C. Sparling, M.I.Ae.S., has been appointed Chief Engineer of the Sperry Gyroscope Co., responsible to **Preston R. Bassett,** F.I.Ae.S., Vice-President in charge of Engineering. Mr. Sparling joined the company in 1915. During his early association with Sperry he worked on engineering design problems in connection with the company's World War I effort and in the special department established to handle ship stabilization problems. In 1920 he was named Gyro-Compass Engineer and supervised the design and development of this product for eighteen years. Mr. Sparling became Manager of Product Engineering in 1938 and in 1940 was named Assistant Chief Engineer.

W. Fred Stewart, M.I.Ae.S., Chief of Structures at Spartan Aircraft Co. since June 1938, has been made Executive Engineer in charge of the Engineering Department of the company. He originally joined Spartan in 1936 as Chief Inspector.

David G. Stone, Technical Member, recently a Draftsman with the Airplane Division (Buffalo Plant), Curtiss-Wright Corp., has joined the staff of the N.A.C.A. as a Junior Engineer at the Langley Memorial Aeronautical Laboratory.

Herman R. Sussman, Technical Member, is now teaching Aviation Mechanics at the Air Corps Technical School, Chanute Field. Mr. Sussman has had several years' experience in teaching mechanical subjects, including recently organized Defense Training courses serving employees and apprentices of the Grumman Aircraft Engineering Corp.

Herbert V. Thaden, A.F.I.Ae.S., is Vice-President in charge of Manufacturing for Duramold Aircraft Corp., with headquarters at their office in New York City. He joined this company earlier in the year as Manager of the Commercial Department.

J. A. Vendrell, Technical Member, until recently an Apprentice Engineer with Pan American-Grace Airways in Peru, is now at Cochabamba, Bolivia, in charge there of the Maintenance Shops of Lloyd Aereo Boliviano which is being reorganized by Pan American.

Personnel Opportunities

The Personnel Bureau serves individual members, as well as organizations seeking to employ aeronautical specialists. Any member or organization may have requirements listed without charge.

Wanted

The United States Civil Service Commission announces open competitive examinations for the following positions with the Civil Aeronautics Administration: *Ground School Supervisors*, $2900 and $3500 a year; *Flight Supervisors*, $3200 and $3800 a year; *Maintenance Supervisors*, $2900 and $3500 a year; *Assistant Airway Traffic Controllers*, $2300 a year. Applications may be filed until further notice with the U.S. Civil Service commission, Washington, D. C.

Wanted

Engineers. Experience in aircraft desirable but not essential if otherwise qualified. *Group Engineers, Layout Draftsmen, Stress Engineers, Weight Engineers, Aerodynamicists, Lofting Engineers.* Excellent opportunities for advancement. If you are not employed in Defense work, write or wire: McDonnell Aircraft Corporation, Lambert-St. Louis Municipal Airport, Robertson, Missouri.

Available

Young aeronautical engineer with two and a half years' experience in military aviation wishes to become associated with either a consultant or consulting engineering group in the Philadelphia area, doing design or development work in aeronautics. B.S. in M.E. (Aero. option), Associate Aeronautical Engineer. Address reply to Box 144, Institute of the Aeronautical Sciences.

Student Branches

The Aeronautical University. At a meeting held on October 21, officers were elected as follows: Clifford Beddoes, Chairman; Herbert Reed, Vice-Chairman; Stewart Durrant, Secretary-Treasurer; and Robert Stebley, Instructor in Aeronautical Engineering, Honorary Chairman. Two films were shown at a later meeting held on November 18: "Wings of Steel" and "Aviation Cadet Training" both of which are U.S. Army Air Corps films.

Agricultural and Mechanical College of Texas. Walter S. Weisemann, Jr., Houston representative of American Airlines, at a meeting held on November 13, gave an illustrated talk on the activities of American Airlines at LaGuardia Field. On October 23, the Pan American Airways film on Hawaii was shown. Both meetings were attended by over 120 members.

Boeing School of Aeronautics. Lester G. Kelso spoke on Prof. F. K. Kirsten's cycloidal propeller at a meeting held on October 8, presided over by Chairman Tuthill. A general business meeting was held on October 22.

Casey Jones School of Aeronautics. The Second Annual Banquet was held on November 27. Chairman William Thomas presented I.Ae.S. student membership emblems to nineteen new student members.

University of Cincinnati. Officers for the school year 1941–42 are as follows: Robert Tripp, Chairman; Monroe Duke, Vice-Chairman; Thomas Tripp, Secretary; and Bruce Hartman, Treasurer.

Duke University. A new Student Branch of the Institute was formed at Duke University on November 27. Officers were elected as follows: Robert J. Korstian, Chairman; Murray F. Rose, Vice-Chairman; and James L. Fisher, Jr., Secretary-Treasurer. J. Hoffer, Instructor in Aeronautical Engineering, is Honorary Chairman.

Lawrence Institute of Technology. At the first meeting of the school year, held on October 10, new officers were elected as follows: Frank Hoernschemeyer, Jr., Chairman; Guy Williams, Vice-Chairman; and Alfred Bieman, Secretary-Treasurer. Randall Chapman, Head of the Department of Aeronautical Engineering, is Honorary Chairman.

Massachusetts Institute of Technology. Chairman Ronald Shainin presided at a meeting held on October 22 and spoke briefly on the aims and activities of the Institute. Later, an N.A.C.A. film was shown on the Langley Field wind tunnels. At a meeting held on November 19, Prof. Otto C. Koppen, described the two-control airplane the "Skyfarer" which he designed. Thomas D. Perry of the Resinous Products & Chemical Company spoke on aircraft plywood and adhesives at a later meeting.

University of Minnesota. A meeting was held on October 28 at which Prof. B. J. Robertson gave a talk on superchargers and their application to aircraft. The members of a secondary C.A.A. flight training class were guests at this meeting.

Oregon State College. Chairman L. Robertson presided at a meeting held on October 22. Robert Needham and Bruce Mercer spoke on the "Pro and Con of Side-by-Side or Tandem Trainers."

Rensselaer Polytechnic Institute. At the third meeting of the school year, held on October 30, a motion picture film on "The Story of the Airship and the Goodyear Air Fleet" was shown. It was followed by a talk on "The Airship as a Vital Part of National Defense" by Lt. W. J. Keene who is on leave from the Lakehurst Naval Air Station.

Ryan School of Aeronautics. New officers were elected as follows at a meeting held on October 3: H. G. Hitchcock, Chairman; T. E. Bird, Vice-Chairman; and T. B. Johnson, Secretary-Treasurer. Stanley H. Evans, Director of Engineering, continues as Faculty Sponsor and Honorary Chairman. At a dinner meeting held on October 17, Earl D. Prudden, Vice-President of the School and the Ryan Aeronautical Company, presented Certificates to the winners of the I.Ae.S. Student Branch Lecture Award, Messrs. R. F. Cerna and G. Crowther for their paper on "Preliminary Airplane Design." Later, T. B. Johnson read a paper on "Flying Boat Design."

University of Texas. The formation of this new Student Branch of the Institute took place on October 22. At a later meeting, held on October 27, officers were elected as follows: Harold T. Johnson, Chairman; Robert C. P. Jackson, Vice-Chairman; Rubin E. Kappler, Secretary; and W. S. Chenault, Treasurer. Prof. M. J. Thompson is Honorary Chairman.

Changes in Membership

The following changes in the membership of the Institute have occurred since the publication of the previous issue of the Journal.

Elected to Member Grade

Berger, Emric William, Production Engineer, Consolidated Aircraft Corp.

Bodemeijer, Dirk, Inspector, Netherlands Purchasing Commission.

Greene, Carl Franklin, Col., U.S.A.; Liaison Officer, Materiel Div., Air Corps, at Langley Mem. Aero. Lab., N.A.C.A.

Kocher, Addis Edward, Asst. Executive Engineer, Eclipse Aviation Div., Bendix Aviation Corp.

Peters, William Hart, S.M. in M.E.; Structural Engineer, Airplane Div. (Buffalo Plant), Curtiss-Wright Corp.

Serrallés, Juan Klein, Ae.E.; Assistant Chief Instructor in charge of the Spanish Division, Casey Jones School of Aeronautics.

Tsongas, Alexander, B.S. in Ae.E.; Acting Chief Engineer, Stinson Aircraft Div., Vultee Aircraft, Inc.

Transferred to MEMBER Grade

Locke, Frederick William Sullivan, Jr., M.E.; Research Asst., Experimental Towing Tank, Stevens Inst. of Technology.

Molloy, Richard Clair, S.B. in Ae.E.; Aero. Engineer, Research Div., United Aircraft Corp.

Scoles, Albert Buddy, M.S. in Ae.E.; Lt. Comdr.; Asst. Chief Engineer (Materials), Naval Aircraft Factory, Philadelphia.

Elected to Technical Member Grade

Campbell, Forrest, Jr.; Layout Draftsman, Waco Aircraft Co.

Clark, Clayton Lincoln, B.S. in E.E.; Aircraft Inspector, U.S. Army Air Corps, at Consolidated Aircraft Corp.

Diver, John R., S.M.; Aero. Engineer, Aeroproducts Div., General Motors Corp.

Dodd, Lavon Couch, B.S. in E.E.; Senior Electrical Layout Draftsman, Lockheed Aircraft Corp.

Haifter, Mitchel, M.E.; Ae.E.; Capt., Air Corps, U.S.A.; Base Engineering Officer, Hq. & Hq. Sq., 36th Air Base Group, Jackson Army Air Base, Mississippi.

Haig, Chester Raymond, Jr., M.S.; Engineer, Fairchild Aircraft Div., Fairchild Engine & Airplane Corp.

Hitch, Robert Arthur, M.S. in M.E.; Draftsman, The Glenn L. Martin Co.

Hubbard, John Dean, B.S. in M.E.; Structural Engineer, Vought-Sikorsky Aircraft Div., United Aircraft Corp.

Jacobs, Maurice David, M.Ind.Ed.; Asst. Instructor, Air Corps Technical School, Chanute Field.

Johnson, John Osborn, Asst. to Contract Administrator, North American Aviation, Inc.

Lentz, Ralph Godfrey, Design Engineer, Allied Aircraft Corp.

McClain, Thomas Hugh, Junior Research Engineer, Lockheed Aircraft Corp.

Mack, Fred Joseph, Jr., Layout Draftsman (Power Plant). The Glenn L. Martin Co.

Matthews, Francis Dukehart, S. B.; Instructor, Boeing School of Aeronautics.

Miller, Marsh Weston, Jr., B.A.; Ensign, U.S.N.R.; Navigation Officer, Patrol Squadron 101, Cavite, P. I.

Newman, Clyde Alexander, B.S. in E.E.; Senior Layout Draftsman, Lockheed Aircraft Corp.

Roffelsen, Harry J., Engineering Instructor, Casey Jones School of Aeronautics.

Saltzman, Ernest Clifford, B.S.; Jr. Aero. Engineer, Materiel Div., U.S. Army Air Corps, Wright Field.

Seltzer, Leon Zee, B.S.E.; Asst. Prof., Aero. Engineering, Virginia Polytechnic Institute.

Shaw, Samuel Stiles, Factory Manager, General Aircraft Corp.

Skoglund, Victor John, M.S.; Project Engineer, Pratt & Whitney Aircraft Div., United Aircraft Corp.

Williford, David Parsons, B.S. in Ae.E.; Aero. Engineer, Boeing Aircraft Co.

Transferred from Student Member to Technical Member Grade

Anderson, Warren Gene, S.B. in Ae.E.; Research Asst., Mass. Inst. of Technology.

Berry, John Raymond, Jr., B.S. in Ae.E.; 2nd Lt., Junior Engineer, U.S. Army Air Corps, Materiel Div., Wright Field.

Cantwell, Raymond Anthony, Student, Tri-State College.

Chandler, Roger Lowell, B.S. in M.E.; Draftsman, Boeing Aircraft Co.

Cherniak, George Sadwin, B.S.; Research Asst., Mass. Inst. of Technology.

Cherwony, Alexander, B.Ae.E.; Detail & Design Draftsman, Airplane Div. (Columbus Plant), Curtiss-Wright Corp.

Coe, John Moment, B.Ae.E.; Stress Analyst, Grumman Aircraft Engineering Corp.

Cole, Charles Willard, Stress Engineer, Boeing Aircraft Co.

Cone, Douglas Beebe, B.Ae.E.; Engineering Trainee, Lockheed Aircraft Corp.

Davis, Craig Carlton, Jr., B.S. in G.E.; 2nd Lt., U.S. Army Air Corps, Wright Field.

DeWitt, Robert Morrall, B.Ae.E.; Engineer on Experimental Blade Design, Hamilton Standard Propeller Div., United Aircraft Corp.

Epstein, Aaron, B.S. in M.E.; Jr. Stress Analyst, Consolidated Aircraft Corp.

Fay, Gerald William, B.Ae.E.

Gentle, Ernest James, B.S. in C.E.; Sr. Design Engineer, Lockheed Aircraft Corp.

Grenzeback, Robert James, B.S. in M.E.; Teaching Asst. in Mech. Engineering, University of California.

Grottle, Albert C., B.S. in Ae.E.; Apprentice Engineer, Pan American Airways System.

Hannifin, Everett, B.S. in Ae.E.

Harmer, Harold J., B.S.; Jr. Engineer, Landing Gear Stress Dept., Bendix Aviation Corp.

Harper, John Joseph, B.S. in M.E.; Grad. Asst., Georgia School of Technology.

Hawley, Edwin Riley.

Healy, Donald V., B.Ae.E.; Engineer, Vought-Sikorsky Aircraft Div., United Aircraft Corp.

Hughes, Eugene Howard, Junior Detailer, Lockheed Aircraft Corp.

Hunt, Donald Casey, B.Ae.E.; Procurement Inspector—Aircraft Engines, U.S. Army Air Corps.

Hunton, Fred Wilson, B.S. in Ae.E.; Asst., Engineering Metals Lab., Mass. Inst. of Technology.

Lecavalier, Fernand, S.B. in Ae.E.; Jr. Engineer, National Research Council, Canada.

Lee, Joseph C., C.E.; Draftsman, Lee Engineering Co.

Maller, Monroe Alvin, B.S. in Ae.E.; Aero. Engineer, Consolidated Aircraft Corp.

Maloney, Philip Robert, Ae.E.; Aircraft Inspector, Consolidated Aircraft Corp.

Matzenauer, James Otis, B.S. in Ae.E.; 2nd Lt., Design Development Engineer, U.S. Army Air Corps, Wright Field.

Oppenheim, Harold Everett, B.Ae.E.; Aero. Engineer, Curtiss Propeller Div., Curtiss-Wright Corp.

Pollock, Robert Thomas, Jr. Engineering Inspector, Consolidated Aircraft Corp.

Preston, Arthur Dale, Aircraft Inspector, Consolidated Aircraft Corp.

Rumsey, Charles Bertrand, B.S. in M.E.; Grad. Asst. in Mech. & Engineering Drawing Dept., Georgia School of Technology.

Samson, David P., Jr., Draftsman, The Glenn L. Martin Co.

Schaefer, William Henry, B.S. in Ae.E.; Stress Analyst, Consolidated Aircraft Corp.

Schoch, Edwin Foresman, B.S. in M.E.; Aviation Cadet, U.S.N.R.; U.S. Naval Air Station, Jacksonville.

Scott, Benjamin Clyde, Jr., S.B. in Ae.E.; Structures Dept., Airplane Div. (Columbus Plant), Curtiss-Wright Corp.

Smisko, Andy, Meteorologist, United Air Lines Transport Corp.

Stamy, James Leland, Sgt. Instructor, U.S. Army, Camp Claibonne, La.

Stivers, Louis Scott, Jr., M.S. in Ae.E.; Aerodynamics Dept., Douglas Aircraft Corp.

Trigg, Leslie John, B.S. in Ae.E.; Propeller Engineer, Hamilton Standard Propellers Div., United Aircraft Corp.

Tulpan, Theodore Frank, The Glenn L. Martin Co.

Voyles, James Homer, Jr., B.S. in G.E.; 2nd Lt., Experimental Engineering Section, Materiel Div., U.S. Army Air Corps, Wright Field.

Watson, Douglas Courtenay, B.Ae.E.; Project Engineer, AGA Aviation Corp.

Weiss, Edward Lionel, Draftsman, Platt-LePage Aircraft Co.

Wellman, Roy Joslyn, M.E.; 1st Lt., U.S. Army Air Corps, Wright Field.

Wells, Roy O'Niel, B.S. in M.E.; Draftsman, Douglas Aircraft Co.

Wright, Philip Clare, Junior Inspector, Consolidated Aircraft Corp.

Yager, Leland Reyman, B.Ae.E.; Jr. Flight Engineer, Pan American-Grace Airways, Inc.

Yudewitz, Samuel, M.Ae.E.; Engineer (Structures), Airplane Div. (Columbus Plant), Curtiss-Wright Corp.

Meeting of Philadelphia Section

Joint Session with Franklin Institute

A meeting of the Philadelphia Section was held at the Franklin Institute on November 5 and 6. The first session on the evening of November 5, a lecture sponsored jointly by the I.Ae.S. and the Franklin Institute, was preceded by a reception and dinner to the lecturer, Dr. Willard F. Bartoe. Mr. Walton Forstall, Vice-President of the Franklin Institute, opened the session. The following is a summary of the paper presented.

Some Observations on the Military Service Requirements of Transparent Plastics.

Dr. Willard F. Bartoe, *Physicist, Röhm & Haas Co.*

For best optical qualities, transparent plastics must be used in such a way that all optical paths through the material are perpendicular to the surfaces. As the angle of incidence increases, reflection losses at both surfaces reduce the light transmission. When the angle of incidence is as great as 75° for example, light transmission is reduced 45 per cent. Shape of the section also affects optical qualities since bending the sheet naturally exaggerates the prismatic effect of normal thickness variations. Flat sheets will give best optical service; simple spherical or cylindrical sections rate a close second, presuming that sighting is done from the center of curvature; combinations of cylindrical and spherical section are optically the least desirable.

High localized surface stress concentrations will cause "crazing" (minute fissures on the surface) of all types of transparent plastics, especially when the plastics are exposed to weather. Obviously, materials that fail relatively rapidly on exposure without applied external stress will not be so apparently affected by such stresses as materials (such as cast acrylic plastics) which do not exhibit spontaneous failure. Such high localized surface stresses must be avoided, however, if maximum optical permanence is expected of any plastic.

The tests described in this paper were made on the cast acrylic resin plastic manufactured under the trade name "Plexiglas." It was found to be resistant to shattering by bullet impact. Any proper installation under normal conditions can be expected to withstand everything except the repeated impact of larger caliber bullets. This commercial acrylic resin plastic is not appreciably embrittled by temperatures as low as −70°F. It is believed that this cannot be claimed for other types of plastic.

It will function satisfactorily in pressurized cabin enclosures if care is taken to prevent concentrated bending stresses being set up in the plastic by the air pressure load. This can be done by using cylindrically and spherically curved sections (or their combinations) and so mounting these sections that the air pressure forces will be resolved into essentially tensile stresses in the plastic sections.

Sessions of Philadelphia Section

On November 6, a morning and an afternoon session of the Philadelphia Section were held. E. Burke Wilford, Chairman, and Ralph H. McClarren, Secretary, who were responsible for arranging the program, presided at these sessions. The papers presented are summarized below.

Physiological Limitations to the Performance of Aircraft

Dr. Carl F. Schmidt, *Pharmacology Laboratory, School of Medicine, University of Pennsylvania*

The speaker reviewed the effect of four factors limiting the full use of the high-speed maneuverability, rate of climb and ceiling of which military planes are now capable: (1) Cold, at temperatures as low as −40° to −60°F., which cannot adequately be combatted by flying suits that are too bulky or by electrically heated clothing which draws upon the plane's power reserve and would lead to serious results upon failure at high altitude. (2) Oxygen lack leading to effects similar to acute alcoholism (and ultimately unconsciousness and death), which begin at about 10,000 feet, but can be successfully combatted by oxygen inhalation apparatus up to about 30,000 feet. Above this height, oxygen has to be administered under pressure, since at 50,000 feet the atmospheric pressure is less than the tension of water vapor and carbon dioxide in the lungs, making it impossible for any oxygen to be absorbed by the lungs at this pressure. (3) Reduced barometric pressure, not only contributing to oxygen lack but also to discomfort from expansion of gases trapped in body cavities and the acute condition known as the "bends." The latter is assumed to be due to the release of nitrogen emboli in blood and tissues but there seems reason to regard this as a not wholly adequate explanation, since aero-embolism occurs under varying conditions depending on rate of ascent, length of stay at high altitude and the relation to an average critical altitude of 25,000 feet, below which it will not occur. (4) Centrifugal force, sometimes exceeding 10 g., as in a quick pullout from a fast dive, which causes a sudden decrease in blood pressure and the blood supply to the brain, bringing on visual and mental "blackout." Dive bombers are equipped with flaps to reduce the speed of the

dive and experiments with the pilot in a prone or crouching position have been tried to reduce the sudden flow of blood away from the heart and brain at the moment of the pullout. The pressurized, heated airplane cabin with oxygen supply is believed to be the best solution for the first three problems at altitudes above 20,000 feet, although the added weight of such installation and dangers attendant on its failure are deterrent factors. "Blackouts" due to centrifugal force remain a serious problem.

Design and Manufacture of Hollow Steel Propeller Blades

H. P. Reiber, *Quality Engineer, Blade Plant, Lycoming Div., Aviation Corporation*

Description of manufacture of propeller blades from seamless cold-drawn tubes of Nickel-Chromium-Molybdenum steel SAE 4330-X. An internally polished tube swaged and flanged on the shank end is lathe turned to proper wall thickness (increased for one edge) on a mandrel. A diaphragm is welded into the large open end and rust inhibited water injected through a pipe connection at the flange end and maintained under pressure while the tube is bent to a curvature such that the convex edge will provide a seamless leading edge. While still cold and filled with water, the bent tube is partially flattened, then the diaphragm removed, water drained, the sheared end (toward the tip) welded and a forked locater attached. Next the flattened tube is hot preformed to blade shape between hot dies on a hydraulic press, the locater and shank flange registering the tube in proper position. At the proper moment, inert gas is forced into the tube under high pressure, inflating it in the dies to create blade shape. The trailing edge, tip, and part of the tip section leading edge is resistance seam-welded. The locater and triangular position of the trailing edge are removed to a rough approximation of finished plan form. Copper wires are then inserted through the shank inside the blade along the leading and trailing edges. By heating in a controlled atmosphere furnace, copper filleting is created which eliminates stress raisers at the end of the weld. The welded and brazed blade is heated and registered between cold dies. High pressure inert gas inflates the blade to an exact duplicate of the die cavity in combination with the die closing operation, thus achieving guaranteed duplication and dimensional tolerances. (The full text and figures for this paper are being prepared as an illustrated lecture for early circulation to all Institute Sections and Student Branches.)

Substitution of Steel for Aluminum

Horace C. Knerr, *Metlab Co.*

American steel production for 1941 is estimated at 86 million tons, or nearly 300 times that of aluminum. Alloy steel may be around 20 million tons. Total aluminum represents about $1^1/_2$ per cent of this amount.

Although steel is scarce, present potential resources of manufacture and working are vast as compared with aluminum. Partial substitution of steel for aluminum may be found necessary or advisable for aircraft production.

Taking representative values for wrought magnesium and aluminum alloy, and alloy steel, it is found that they have about the same strength-weight factor.

Steel lends itself to acetylene and electric welding instead of riveting. Overlapping is avoided, joints are stiffer, whereby more weight is saved. Direct substitution of one metal for another is, of course, seldom practicable. Design must take into consideration many factors including fabricating methods, joining, stiffness, corrosion resistance, fatigue, and the like.

Steels have improved during the last decade, the alloy 4340X offering distinct engineering advantages over the commonly used 4130X. Elastic modulus is a controlling factor in many items of design, but, steel equals aluminum when each is in the form of a (hollow) section having the maximum moment of inertia. Aluminum alloy is especially favorable for surfaces and for structural parts of small planes. The advantages of steel for beams and wing spars inherently increase with the size of the airplane.

Tubular alloy steel wing spars of complex shape and in sections as long as 24 feet have been successfully heat treated without distortion. Tensile strength values as high as 180,000 lbs. per sq. in. were used. Substitution of steel for aluminum castings is much more difficult than for wrought sections. It is reasonable to suppose that the substitution of alloy steel wherever applicable would permit the saving of 10 to 25 per cent of aluminum alloy now required for military aircraft, to be conserved for more manufacture in locations where no substitution is practicable.

Summary of Rotating-Wing Aircraft Development

E. Burke Wilford, *President, Pennsylvania Aircraft Syndicate, Ltd.*

The speaker showed films on flights of the Pitcairn "Whirl Wing," the Kellett Army Giroplane and the Sikorsky Helicopter. The latter was shown equipped with floats and operating over a body of water—taking off, hovering, straight and turning flight and landing.

Determination of Airplane Critical Altitude by Flight Tests

L. C. Miller, *Brewster Aeronautical Corp.*

The full text of this paper will be published in an early issue of the Journal.

Productive Education

John Rogers, *Director and Senior Instructor of Army Training, Rising Sun School of Aeronautics*

The speaker pointed out that the increases in the number of certified mechanics from 8993 in 1930 to 11,177 in 1940 had not kept pace with the rate of increase in production for this period, i.e., 650 military aircraft per year to approximately 8000 per year and factory employment from 8000 to 125,000 workers; that this situation was particularly serious in view of reliably estimated requirements of 225,000 workers by the end of 1941 and 340,000 for 1942. He described the methods of selecting those applicants who could be most thoroughly and quickly trained as mechanics for inspection, maintenance, repair, overhaul and manufacturing: the Humm-Wadsworth scale for determining temperament or "personality traits"; aptitude tests for determining hand-and-eye coordination and the sense of spatial relationships such as the Minnesota Manual Dexterity Tests; the tests for special skills such as the written and manual operations tests set up by the Lockheed company for proving an applicant's actual familiarity with the skills claimed; and general intelligence tests, such as the Otis tests of Mental Ability and the revised Army Alpha Tests, to determine whether the applicant has too much or too little intelligence for the job sought. In the training given in private schools, public schools, Army schools and the numerous factory courses in preliminary and progressive training, he emphasized the use of cutaway models, mock-ups, wall diagrams, lantern slides and motion pictures, particularly to familiarize the student with the latest equipment and products which would not be made available to the schools. He described a type of blackboard chart, outlined by a perforated imprint, invisible to the student, which the instructor could fill in, step by step, with colored chalk to illustrate the development of the subject under discussion.

Establishment of Aircraft Instrument Production in the New Philadelphia Plant

W. A. Reichel, *Director of Engineering, Pioneer Instrument Div., Bendix Aviation Corp.*

In expanding production twenty-fold in two years in such a highly specialized field, training and handling of personnel is of paramount importance. In providing a completely air-conditioned 60,000 square foot area inside a larger factory building

of old style construction, the hollow tile insulating walls were provided at intervals with double plate glass windows to avoid any development of claustrophobia among personnel working in this area. Engineering personnel for the new factory was recruited from among engineers already resident in the region who were sent to the main plant in Bendix, N. J., for preliminary training. Some skilled workers, who had to be transferred from Bendix to provide the nucleus of a production organization and train new workers, were enabled to carry on their work without interruption through the special assistance given them in establishing living arrangements in the new community.

Special tooling equipment, simplified production, assembly and inspection methods created more simple, repetitive operations which could be done by girls after very brief training periods. Music over an amplifying system will be used to counteract the monotony of certain types of work. Production is carried on satisfactorily although over 40 per cent of personnel is unskilled.

Unique Economical Production Methods in the Aeronautical Industry

Joseph S. Pecker, *Consultant o The Machine and Tool Designing Co., Philadelphia*

Review of sheet metal stamping processes: the Guerin method, with press having a thick pad of rubber on the upper ram and a nest of blank dies of steel mounted on a plate movable onto roller tables surrounding the press, so that no time is lost in stripping the blanks and scrap from one die nest while another is loaded into the press; use of rubber strips on top and bottom of press in piercing and blanking operation to float out the blank and strip the scrap when large quantities of pieces are to be made; use of plow steel and Kirksite zinc alloy for dies in this process which are easily machined and do not need hardening; use of rubber pads 12 inches thick for forming blanks around the sides of a die, which can be shaped at inward angle on the sides to allow for spring-back in the metal; use of "Cerrobend" and "Cerromatrix" for economically making dies, as used in cylindrical draw stampings, directly from the wooden pattern; magnetic method for holding highly diamagnetic Cerromatrix dies in press, permitting easy removal; use of Whistler universal perforating die for piercing various sheets without expense of special die for each different type; method of using Cerrobend with low melting point of 160°F. as filler in the bending of thin-walled tubes so that it will show up any imperfections in the tube and can be removed easily after bending; use of Cerromatrix to mold nesting blocks for assembly fixtures. (This paper will be made available as an illustrated lecture for Sections and Student Branches.)

Philadelphia Section Dinner

The meeting was concluded with an informal dinner on the evening of November 6 at the Hotel Belgravia. Francis G. Tatnall, Manager of the Testing Machine Dept., Baldwin-Southwark, was toastmaster. The speakers were Frank W. Caldwell, President of the Institute, Captain E. W. Pace, U.S.N., Manager of the Naval Aircraft Factory, Major Leigh Wade, U.S. Army Air Forces, who spoke on "Aviation in South American Defense," and William Courtenay, Aviation Editor of the London "Daily Sketch," who described "The Battle of Britain."

The Technical Information Service
of the
Institute of the Aeronautical Sciences

This service has experienced personnel under the supervision of trained aeronautical engineers to compile any information desired. The services range from listing specialized reference books to the preparation of exhaustive bibliographies, digesting of reports and general surveys of any aeronautical subject.

Some of the available services are:

Bibliographies on any aeronautical subject.

Reports on any aeronautical subject.

Digests of aeronautical books, papers, periodicals and references.

Translations in all languages.

Engineering investigations of special aeronautical subjects.

Biographies of individuals engaged in aeronautics.

Photostats of any aeronautical or general engineering material.

Microfilms made on special order.

Photographs made from the Institute's photographic collection.

Drawings and tracings made.

In addition to the services mentioned any commission which comes within the scope of the Service will be accepted.

Research work is charged at the usual library fee of $2.00 per hour. Special arrangements may be made for work requiring several weeks or months.

Translators are available for accurate transcriptions of all foreign language data. Translations are carefully edited by trained engineers at the standard rate of 1¢ per word. Minimum charge, $2.00.

Reproductions of any material in the Aeronautical Archives of the Institute may be ordered at standard photostat rates.